ENGINEERING BROWN ADIPOSE TISSUE

by

Annemarie McCartney

A dissertation submitted to Johns Hopkins University in conformity with the requirements for the degree of Doctor of Philosophy

Baltimore, Maryland

July, 2016

ABSTRACT

Research on brown adipose tissue has been conducted largely through analysis of adipocytes grown in monolayer. However, studies of other cell types that have been cultured in 3-dimensional scaffolds using tissue engineering techniques have shown that cell morphology can influence cell behavior, including differentiation. In the present study, we used synthetic hydrogels to support 3-dimensional adipogenesis of adipose-derived stem cells, modifying the scaffold properties to optimize brown adipogenesis. Beyond measuring expression of brown adipose-specific genes and proteins, we characterized the adipocytes' mitochondrial respiratory profiles to assess cell function. White adipose-derived stem cells that underwent brown adipogenesis had dramatically different respiratory profiles in monolayer culture compared to 3-dimensional culture, and this was true for both rat and human cells. Further, the rat and human adipocytes displayed opposite functional phenotypes, suggesting that rat data cannot be extrapolated to the human condition in this case. Our synthetic brown adipose tissue, made from human white adipose-derived stem cells, can be used to study cell biology, to test pharmaceuticals, and potentially to translate to *in vivo* use as a metabolic sink.

Readers: Dr. Luis Garza and Dr. Guang William Wong

ACKNOWLEDGEMENTS

To Dr. Jennifer Elisseeff, thank you for your support and patience and for giving me the freedom to innovate.

To Jessica Yang, thank you for your assistance with the PCR data and for singing cheesy songs with me in lab.

To the entire Elisseeff lab, thank you for all for helping create an environment where we could all learn from and share with each other, and thank you for sharing my enthusiasm for cake.

To Dr. Luis Garza, thank you for your guidance regarding my Ph.D, M.D., career, and life, as well as your helpful feedback about my thesis.

To the CMM program, especially Dr. Rajini Rao, Colleen Graham, and Leslie Lichter, thank you for your encouragement and support.

To the MD-PhD program, especially Dr. Bob Siliciano, Dr. Andrea Cox, and Sharon Welling, thank you for welcoming me into the Hopkins Family and being such fabulous advocates for me over the years.

To my family and friends, thank you for loving me and keeping me smiling through the ups and downs of this journey.

TABLE OF CONTENTS

LIST OF FIGURES

INTRODUCTION

Tissue engineering

Biomaterials have been used in medicine for decades, serving as implantable devices for bone repair and heart valve replacement, as well as being used as resorbable sutures (Hench and Polak, 2002). However, for prosthetic applications, it is clear that the biomaterials degrade over time without encouraging *in vivo* repair of the defect. Tissue engineering has given hope to regenerative medicine, leveraging three-dimensional scaffolds to support cells, possibly in the presence of exogenous growth factors, in the attempt to create artificial tissues (Rehfeldt et al., 2007). Three-dimensional (3D) *in vitro* models of tissues are important for understanding how cells develop and interact both with each other and their environment. Although many cell biology experiments are conducted on cells cultured in monolayer, the biological function of cells can be altered based on their morphology (Stevens and George, 2005; Rehfeldt et al., 2007; Breuls et al., 2008; Mazzoleni et al., 2009). Therefore, growing cells in a 3D scaffold can be a better model of their *in vivo* function.

A scaffold provides 3D structural support to cells and allows 360° of cell-cell interactions, which is impossible for cells grown in monolayer. Further, the ability to tune the mechanical properties of synthetic polymers has made it possible to create stiff environments conducive to osteogenesis and soft environments for adipogenesis. Beyond understanding cellular function, 3D models can be used as artificial tissues for testing disease models and interventions (Mazzoleni et al., 2009). When considering implanting

engineered tissues into animals, one must consider biocompatibility and degradation. As foreign objects risk being encapsulated rather than integrated by the body, understanding the nature of the scaffold material and the body's reaction to it is vital for translational research. Scaffolds should be biocompatible and biodegradable, but beyond the basic requirements, nuances of scaffold properties, such as stiffness and adhesion, can influence cell behaviors like survival, growth, differentiation, and deposition of extracellular matrix (ECM). Although there is much literature discussing those outcomes, little has been mentioned with regard to the influence of the scaffold on cell respiration. Comparatively more work has been done on cell metabolism in monolayer.

Synthetic polymers

The extracellular matrix (ECM) is comprised of proteins secreted by cells, and the matrix can steer cell differentiation through both physical interactions and soluble proteins. At their best, scaffolds attempt to mimic native ECM, and there are a variety of synthetic molecules and techniques used to make scaffolds. Polylactic acid (PLA) is often used to encourage osteogenesis and chondrogenesis as it is a stiff biodegradable polymer, and polyacrylamide is so tunable that it can make both soft gels and rigid scaffolds (Rehfeldt et al., 2007). Polycaprolactone degrades very slowly and is used for applications that desire scaffold stability (Kang et al., 2007). Our lab has experience with poly(ethylene glycol) diacrylate (PEGDA), a hydrophilic polymer with acrylate functional groups that allow polymerization in the presence of a photoinitiator and ultraviolet light. PEGDA

hydrogels are soft and do not encourage cell adhesion, and our lab has used them to differentiate stem cells (Yang et al., 2005; Hillel et al., 2009).

Extracellular matrix

ECMs can be created from decellularized whole tissues or made from collagen, elastin, fibrinogen, laminin, or a mix of proteins that are present in natural ECM (Rehfeldt et al., 2007). These scaffolds are biocompatible but may not always be appropriate for use in humans, particularly if derived from animals (Stevens and George, 2005). von Heimburg and colleagues (2001) created porous "sponges" made from bovine collagen fibers and seeded them with human primary preadipocytes. They implanted the sponges in immunocompromised mice, and after several weeks found blood vessels on the surface of the sponge and mature adipocytes penetrating into its surface. Undifferentiated preadipocytes had penetrated further into the sponge, but the authors assumed that the pore size of the scaffold was too small to accommodate adipogenesis.

Some researchers experiment with drug delivery systems and cell-free scaffolds in the attempt to encourage *in vivo* tissue regeneration and eliminate the need for delivery of exogenous cells. Matrigel is a mix of basement membrane proteins and growth factors secreted by cancer cells, and it can encourage adipogenesis when injected *in vivo* with the growth factor bFGF. Kimura et al. (2002) created hydrogels that slowly secreted bFGF and implanted them with Matrigel subcutaneously in the mouse back. They found that native cells migrated into the Matrigel and differentiated into adipocytes. Unfortunately,

the exact composition of Matrigel is unknown and can vary, so it is not an ideal substrate for translation to regenerative medicine.

Much of native adipose ECM is composed of collagen, especially collagens IV and VI, and adipocytes remodel the ECM continually (Mariman and Wang 2010). Sharma and colleagues (2011) analyzed the effects of ECM secreted by preadipocytes on activation of metabolic pathways in hepatocytes and compared the results to those with hepatocytes grown in collagen sandwich cultures. The "Adipogel" ECM was rich in fibronectin and collagen IV, which are present in large amounts in native liver ECM, and culturing hepatocytes on it enhanced their synthesis of albumin.

Hydrogels

While ECM is inherently biocompatible, scaffolds made from synthetic polymers can be readily synthesized and their properties can be tuned. A hydrogel is composed of hydrophilic polymers and thus has a high water content that mimics tissue and allows for nutrient transport to cells (Hoffman 2001; Patel et al., 2005; Hillel and Elisseeff, 2010). Photopolymerization of hydrogels using ultraviolet light-sensitive compounds to initiate crosslinking of polymers is a way to encapsulate cells uniformly in gels (Yang et al., 2005). Further, the gel can be injected or shaped in a desired site before polymerization. Our lab examined the toxicity of photoinitiators and determined that Irgacure 2959 is relatively non-toxic across different cell lines (Williams et al., 2005), and we have experience using it to polymerize poly(ethylene glycol) diacrylate (PEGDA) hydrogels. Further, our lab has experience differentiating stem cells into white adipocytes within

biocompatible PEGDA hydrogels and implanting them into animals (Hillel et al., 2009), and in 2010, Hillel and Elisseeff showed improved adipogenesis of embryonic progenitor cells grown in hydrogels versus monolayer.

Use of cell adhesion peptides

The cytoskeleton connects to the ECM via adhesion proteins, and the rigidity of the ECM can determine the types of adhesions formed, as well as influence cell migration and function (Nicolas and Safran, 2006; Rehfeldt et al., 2007). To attempt to guide cell-scaffold interactions, specific peptide sequences can be attached to synthetic polymers (Hench and Polak, 2002; Patel et al., 2005), and they can influence differentiation. The Arg-Gly-Asp (RGD) sequence of fibronectin serves as the attachment site for cell surface integrins. Despite lack of enzymatic activity, integrins can regulate cell signaling pathways, bind growth factors, and lead to activation of growth factor receptors in the absence of growth factor (Ivaska and Heino, 2010). Some important integrins include: α5β1, the fibronectin receptor, which is embryonic lethal when knocked out; α4 is also embryonic lethal; β subunits bind a variety of signaling molecules, including protein tyrosine kinases (Ivaska and Heino, 2010). Although the surface molecules change with time in culture, human adipose-derived stem cells express CD29 (β1 integrin) and CD49 (α4 integrin), among other cell surface proteins (Gimble et al., 2007), and α4 does not need RGD to bind to fibronectin (Ivaska and Heino, 2010). Mouse BAT ASCs express CD29 as well; however, WAT ASCs expressing CD29 did not function the same as those from BAT when both cell types were differentiated to cardiac muscle cells (Gimble et al.,

2007). Mature adipocytes also express β1 integrin (Farnier et al., 2003), and with differentiation, ASCs transition from expressing α5 integrin (receptor for fibronectin) to α6 integrin (receptor for laminin), which regulates cell adhesion and migration (Liu et al., 2005). It is evident that binding of adhesion peptides can regulate cell activity, and our lab has shown that the presence of RGD in a synthetic scaffold can influence differentiation of mesenchymal stem cells (Yang et al., 2005; Singh et al., 2013) and mitochondrial membrane potential of human ASCs (Reid et al., 2013). Kubo et al. (2000) and Mariman and Wang (2010) have described changes in ECM proteins produced by differentiating preadipocytes in monolayer, noting that fibronectin developed early in the culture and degraded over time, and Kubo et al. (2010) surmise that it helps induce adipogenesis while acknowledging that other reports suggest it inhibits differentiation.

Brown adipose tissue

The adipose organ is comprised of white and brown adipose tissue, and both types contain lipid. Although white adipose functions mainly to store excess energy, brown adipose produces heat and is defined by expression of uncoupling protein 1 (UCP1) (Cannon and Nedergaard, 2004).

While white adipose tissue (WAT) is derived from the lateral plate mesoderm, brown adipose tissue (BAT) arises from the central dermomyotome, as does muscle (Richard

and Picard, 2011). Work published in 2007 from Timmons and colleagues used a microarray analysis of 8000 transcripts to create transcriptional signatures from primary brown and white preadipocytes. Their work showed differences in the gene expression between white and brown adipocyte precursor cells, with brown preadipocytes sharing a transcriptional signature with skeletal muscle precursor cells. One of the shared transcription factors, Myf5, was the focus of a lineage-tracing experiment by Seale et al (2008). They used Myf5-Cre knock-in mice with a yellow fluorescent protein (YFP) reporter to show that skeletal muscle and BAT, but not WAT, develop from Myf5-expressing progenitor cells.

Locations in adult

In rodents, BAT is located in interscapular, subscapular, pararenal, and axillary depots (Cinti, 2006; Richard and Picard, 2011). Compared to humans, rodents have a higher proportion of BAT, likely due to increased risk of hypothermia from a greater surface-to-volume ratio, allowing for greater heat dissipation. Further, they live at room temperature or below and require an increased basal metabolic rate to maintain their body temperature. Brown adipose mass increases with cold acclimation and is responsible for nonshivering thermogenesis (Cannon and Nedergaard, 2004).

Although human infants have interscapular BAT similar to that of rodents (Lidell et al., 2013), the tissue disappears with age, and until recent decades it was assumed that adults did not have BAT (Cypess, et al. 2009; van Marken Lichtenbelt and Schrauwen, 2011). However, with the increased use of PET/CT imaging, functional BAT depots have been

identified in adults. The radiotracer ^{18}F-fluorodeoxyglucose (^{18}F-FDG) is a glucose analog that is taken up by metabolically active cells, and it is used frequently to look for metastatic lesions in people with cancer. Many patients had tissue in their neck take up ^{18}F-FDG despite lack of metastases there, and it was hypothesized that those metabolically active sites may represent brown adipose depots. Cypess and colleagues (2009) examined over 3500 PET-CT scans from nearly 2000 patients and analyzed biopsies when available, determining that the PET-CT scans were indeed demonstrating active brown adipose. The most common depots were supraclavicular and cervical, and some patients had paraspinal BAT as well. In the same year, Saito et al. (2009) reported the presence of functional brown adipose tissue in healthy adults who were exposed to cold. They performed PET-CT scans on the same subjects under different conditions and at different seasons of the year, finding increased ^{18}F-FDG uptake in BAT during cold exposure and even more BAT activity during the winter, possibly due to BAT hyperplasia. Like Cypess's group, Saito and colleagues found an inverse correlation between BAT activity and body mass index. van Marken Lichtenbelt et al. (2009) also studied BAT activity during cold exposure, comparing its activity in overweight and normal weight men. They identified active BAT in both groups, and their findings agreed with those of Cypess and Saito, asserting that BAT was less active in men with a higher body mass index. A very small study also published in 2009 by Virtanen et al. analyzed biopsies from three healthy volunteers who demonstrated BAT activity on PET scans. The biopsies revealed cells containing multiple lipid droplets, and the samples were immunoreactive for UCP1. In a study from P. Lee et al. (2011), biopsies of supraclavicular fat were taken from individuals who had active supraclavicular BAT on

PET/CT scan as well as from people who did not exhibit ^{18}F-FDG uptake in that region. Both groups had uncoupling protein 1-positive biopsy samples, and precursor cells isolated from the tissues were able to differentiate into brown adipocytes. This work showed BAT exists even when undetectable on PET/CT and demonstrated inducible brown adipogenesis in humans.

Structure

While white adipocytes have a large, single lipid droplet, brown adipocytes contain multiple, small lipid droplets. Grossly, BAT appears brown, due to rich vascularization and a high number of mitochondria per cell, and thus a large quantity of cytochrome c (Cinti 2006; Richard and Picard, 2011). Uncoupling protein 1 (UCP1), also known as thermogenin, is a mitochondrial carrier protein that spans the mitochondrial inner membrane and is only expressed in brown adipocytes. It can conduct protons across the membrane, dissipating the electrochemical membrane potential as heat (Richard and Picard, 2011). Since the proton-motive force that would otherwise be used by ATP synthase is no longer available with UCP1 activation, UCP1 is said to "uncouple" oxidative phosphorylation.

Function

The primary function of BAT is generation of heat through β-oxidation of fatty acids to create potential energy in the form of an electrochemical gradient across the

mitochondrial inner membrane and subsequent dissipation of the gradient as heat. This creation of heat, called non-shivering thermogenesis (NST), is important for animals that are at risk of hypothermia (Cannon and Nedergaard, 2004). As opposed to shivering thermogenesis, which is heat generation from muscle activity, NST involves activation of brown adipose. Although NST is triggered by cold exposure, it is initiated before shivering thermogenesis, and the rich vascular network within BAT allows for distribution of the heat to the rest of the body.

From an energy conservation perspective, BAT activity "wastes" the energy from the mitochondrial electrochemical gradient, which was created from oxidation of fatty acids. BAT is so "wasteful" that 80-100 grams (about three ounces) of BAT working at only half-maximal capacity can burn about 300 kilocalories per day, which translates to over 30 pounds in a year (Stock and Rothwell, 1983). Interestingly, studies in rodents that lack brown adipose show decreased fat mass and resistance to obesity, except when living in a thermoneutral environment (Richard and Picard, 2011; van Marken Lichtenbelt and Schrauwen 2011). A study from Lowell et al. (1993) examined two different transgenic mice lines, each of which had diminished BAT and increased WAT mass, but one of the strains recovered its BAT mass and attained normal weight. Although the other transgenic line remained obese despite not being housed in a thermoneutral environment, it had developed hyperphagia, so Lowell and colleagues' results may not necessarily contradict data from other BAT-deficient animal studies. This suggests that BAT contributes to basal energy expenditure at thermoneutrality and that NST is more energy-efficient than other means of heat production, such as shivering thermogenesis.

In a study of six healthy young men, Ouellet and colleagues (2012) exposed the subjects to 3 hours of mild cold, designed to minimize shivering. Using PET/CT imaging and calorimetry, they saw increased BAT activation and measured an 80% increase in whole body energy expenditure, translating to an average burn of 250 kcal. The average volume of brown fat activity was 168 mL, and according to van Marken Lichtenbelt and Schrauwen (2011) it is common to note over 100 cm^3 of BAT in PET/CT studies.

Regulation

Adrenergic stimulation is necessary for thermogenesis. Each brown adipocyte is innervated by sympathetic nerves, and activation is controlled centrally by the hypothalamus and brainstem. Upon stimulation, the nerves release norepinephrine at the adipocytes as well as at the surrounding vasculature. (Cannon and Nedergaard, 2004; Richard and Picard, 2011). Activation of the β3-adrenergic receptor induces intracellular metabolism of triglycerides, which produces fatty acids that act as an energy source as well as activate UCP1 (Richard and Picard, 2011), and this process is enhanced by adenosine signaling (Gnad et al., 2014). Although norepinephrine activates all adrenergic receptors, studies using receptor-specific agonists have demonstrated stimulation of thermogenesis only through β3-adrenoreceptor activation (Cannon and Nedergaard, 2004). In work published in 2012, Whittle et al. show that bone morphogenetic protein 8B (BMP8B) potentiates the action of adrenergic stimulation at BAT, as well as increases the sympathetic stimulation of BAT. Mice lacking BMP8B are

obese despite having normal-appearing BAT, and the authors demonstrate that the BAT is less sensitive to adrenergic stimulation.

A result of norepinephrine acting at the β3-adrenergic receptor is activation of a signaling cascade resulting in cyclic AMP formation. The drug forskolin activates adenylyl cyclase to increase intracellular cAMP and induce thermogenesis, and it has been used to stimulate expression of UCP1 and PGC-1α (Seale et al., 2008). Another compound, isoproterenol is a non-selective β-adrenergic agonist that has been used to induce thermogenesis, but it has higher affinity for the β1-receptor (Cannon and Nedergaard, 2004). Crane et al. (2015) found that stimulation of thermogenesis by isoproterenol is diminished by pre-treatment with serotonin. Obesity is associated with increased serotonin, and the authors found that mice that lack Tph1 (tryptophan hydroxylase 1), an enzyme that produces serotonin, are resistant to a high fat diet and their BAT is more active than that of controls. When exogenous serotonin was administered, the Tph1 knockout mice developed glucose intolerance and their BAT did not respond as robustly to a β-adrenergic agonist. The authors also suppressed Tph1 in wild-type mice with a drug, leading to a similar phenotype as the knockout mice, with resistance to high fat diet and increased BAT activity.

Triiodothyronine (T3) activates the ventromedial hypothalamus, stimulating the sympathetic nerves that innervate brown adipose. It also stabilizes UCP1 mRNA transcripts and potentiates the sensitivity of UCP1 to adrenergic stimulation (Carvalho, et al. 1996). Further, J-Y Lee et al. (2012) demonstrated that at supra-physiologic concentrations, T3 administered to white adipose-derived stem cells undergoing white

adipogenesis causes increased white adipocyte respiration, induces UCP1 expression, and stimulates mitochondrial biogenesis, creating a brown adipose-like phenotype.

Agouti-related peptide (AgRP) neurons can regulate BAT through altering gene expression, leading to insulin resistance. Myostatin is upregulated, among other myogenic genes, which Steculorum et al. (2016) determined mediated BAT insulin insensitivity after AgRP stimulation.

Adipose-derived stem cells

Grafting of white adipose has been a common practice in plastic surgery for years, particularly for soft tissue reconstruction and cosmetic enhancement (Hillel and Elisseeff, 2010), and the potential of adipose-derived stem cells is now being realized. Adipose tissue is rich with adipose-derived stem cells (ASCs), which can be differentiated along multiple lineages *in vitro*, including adipose, bone, muscle, cartilage, and more. Adult stem cells avoid the ethical concerns surrounding embryonic stem cells as well as the risk of teratoma formation, and induced pluripotent stem cells can be challenging to create (Mizuno et al., 2012). The abundance of adipose and differentiation potential of ASCs makes them attractive for use in regenerative medicine. The stromal vascular fraction (SVF) of adipose tissue contains ASCs, preadipocytes, fibroblasts, endothelial cells, and other cell types, and ASCs are isolated from adipose via digestion of collagen and centrifugation of the sample. Although ASCs have multiple cell surface markers, there is not yet a definitive phenotype, and as noted earlier, ASCs with similar cell surface molecules but isolated from BAT versus WAT, function differently when differentiation

down the same pathway (Gimble et al., 2007). It can be difficult to distinguish ASCs from fibroblasts, and they have some of the same surface antigens as pericytes (Mizuno et al., 2012). Further, some surface markers, such as CD34, are seen in human ASCs but only in certain strains of rodents and only in a small percentage of BAT ASCs; other surface molecules are depot-specific (Prunet-Marcassus et al., 2006). Analysis of skin connective tissue fibroblasts demonstrates a diverse population of cells, which vary in their commitment to different lineages. Throughout development of the embryo, Driskell and colleagues (2013) observed changes in cell surface markers of fibroblasts. Through lineage tracing, the authors could determine which populations developed into upper dermis versus lower dermis, distinguishing cells that were necessary for hair development from those that would become adipocytes.

As discussed earlier, brown and white precursor cells arise from different lineages, and Timmons et al. (2007) demonstrated different transcriptional profiles with differentiation. While white and brown preadipocytes shares 72% of up-regulated genes and 52% of down-regulated genes, there were significant differences in their gene expression patterns. Notably, brown preadipocytes upregulated mitochondria-related genes and transiently expressed myogenic factors. Further, the group compared the primary white and brown preadipocytes to immortalized white and brown adipocyte cell lines and found significantly different transcriptional profiles.

Relevant genes for adipogenesis

Peroxisome proliferator activated receptor gamma (PPARγ) is a nuclear receptor in adipocytes and activates genes that stimulate adipogenesis, fatty acid uptake and storage, and glucose metabolism. Although it is also present to some degree in macrophages, liver, kidney, and the colon, PPARγ is necessary for normal adipocyte development, and complete lack of PPARγ is lethal early in development (Jones et al., 2005). The role of PPARγ in adipose is illustrated by Jones et al. (2005) with their creation of adipose-specific PPARγ knockout mice, which lacked brown adipose and had diminished mass of white adipose. Interestingly, these mice become hyperphagic but do not gain as much weight as control animals on a high fat diet. In medicine, PPARγ agonists have been used in the form of thiazolidinediones, which are insulin-sensitizing drugs used to treat people with type 2 diabetes and serve to decrease serum glucose and increase adiponectin (Wong et al., 2011). Although they do not directly stimulate thermogenesis, PPARγ agonists can enhance the thermogenic capacity of BAT by inducing brown adipose gene expression (Richard and Picard, 2011).

Other adipose-specific genes include adiponectin and fatty acid binding protein 4. Adiponectin is a hormone secreted specifically by adipose tissue and is involved in regulation of fatty acid oxidation, glucose homeostasis, and insulin sensitivity. It helps prevent vascular dysfunction in diabetes and it decreases with obesity (Wong et al, 2011). Adiponectin knockout mice have decreased browning of subcutaneous WAT in response to chronic cold stimulation, although their BAT function is normal (Hui et al., 2015). Fatty acid binding protein 4 (FABP4), also called adipocyte protein 2, is expressed in adipocytes and macrophages (Hotamisligil et al., 1996) and carries fatty acids (Cannon

and Nedergaard, 2004). Mice null for FABP4 exhibit insulin sensitivity in the setting of diet-induced obesity but are otherwise normal (Hotamisligil et al., 1996).

Relevant genes for brown adipogenesis include PRDM16, PGC-1α, and Cidea. PRD1-BF-1-RIZ1 homologous domain containing protein-16 (PRDM16) is a zinc finger protein that is necessary and sufficient to induce brown adipogenesis and can induce brown adipogenesis in white pre-adipocytes or myoblasts (Kajimura et al., 2010). It activates PGC-1α and PPARγ by binding directly to them (Richard and Picard, 2011), and when expressed in white pre-adipocytes or myoblasts, it suppresses native gene expression programs (Seale et al., 2008). Seale and colleagues (2008) also showed that mice lacking PRDM16 die at a late stage of development, and BAT from PRDM16 knockout embryos had increased lipid, decreased expression of BAT genes, and increased myogenic genes. PPARγ agonists can stimulate brown adipose gene expression in both BAT and WAT, and Ohno and colleagues (2012) determined that this action of the agonists is mediated by stabilizing the PRDM16 protein. The following year Ohno et al. (2013) published work examining regulation of PRDM16 further. They found that euchromatic histone-lysine N-methyltransferase 1 (EHMT1) is an enzyme that is abundant in BAT and interacts with PRDM16 to regulate thermogenesis. The authors knocked down EHMT1 in brown adipocytes, leading to decreased mitochondrial respiration and uncoupling, but when overexpressing EHMT1 in cells, the presence of PRDM16 was necessary to achieve enhanced expression of thermogenic genes.

PPARγ-coactivator-1α (PGC-1α) is a cold-inducible coactivator of PPARγ that interacts with PPARγ and thyroid hormone receptor to induce expression of UCP1 and it is necessary for cold-induced thermogenesis (Richard and Picard 2011). It is expressed in

BAT, cardiac and skeletal muscle, and kidney, and it is involved in regulation of mitochondrial biogenesis and increases oxidative metabolism. Further, to minimize cellular damage from reactive oxygen species, it enhances elimination of ROS by-products (Austin and St.-Pierre, 2012). Mice null for PGC-1α are cold-sensitive and hyperactive, have impaired mitochondrial respiration, and they gain less weight than controls when fed a high fat diet (Lin et al., 2004). Cidea (cell death-inducing DNA fragmentation factor-like effector A) is highly expressed in BAT and plays a role in thermogenesis but is not induced by cAMP (Kajimura et al., 2010). Cidea can also be found in cardiac and skeletal muscle, brain, and lymph nodes (Zhou et al., 2003). Zhou and colleagues (2003) also found that mice lacking Cidea gain less weight than control animals on a high fat diet, and they maintain higher body temperature in cold conditions, but their BAT and WAT do not have a different morphology than that of control mice.

Status of BAT field

Beige/Brite cells

For decades, it has been known that BAT-like cells can be found in WAT depots after chronic exposure to cold (Young et al., 1984), and they also appear in response to PPARγ agonists (Ohno et al., 2012) and β3-adrenergic receptor agonists (Ghorbani et al., 1997). Gnad et al. (2014) also observed browning of WAT with administration of adenosine receptor agonists. These cells express UCP1, have multiple fat droplets, and contain many mitochondria. However, the origin of these "beige" or "brite" cells is unknown. They are not classical BAT, as they do not arise from Myf5-expressing progenitor cells

(Seale et al., 2008). Seale et al. (2011) demonstrated that murine subcutaneous WAT expresses more PRDM16 than visceral WAT, showing that WAT depots vary in their capacity for undergoing brown adipogenesis. Some researchers have shown evidence that these BAT-like cells arise from stem cells, while others suggest that mature white adipocytes transdifferentiate to brown adipocytes (Frontini and Cinti, 2010). With the rising demand for therapies for obesity, these "beige" or "brite" cells have been a topic of interest in the BAT field, and many groups studying BAT via genetic manipulation have demonstrated UCP1 expression in WAT.

In mice that have been engineered to overexpress UCP1 in adipose tissue, driven by the aP2 promotor (aP2-UCP1 transgenic mice), Stefl and colleagues (1998) saw resistance to obesity but intolerance to cold. These mice had atrophied BAT and expression of UCP1 in WAT, and the authors suggested that the UCP1-positive WAT was contributing to energy expenditure but was unable to compensate for heat loss as well as native BAT would in non-transgenic mice. In 1999, Baumruk et al. published data showing that the WAT from aP2-UCP1 transgenic mice was indeed uncoupled, and Rossmeisl et al. (2002) found that the UCP1-positive WAT had increased mitochondrial content.

In 2001, Cederberg et al. showed that in transgenic mice that express FOXC2 specifically in BAT and WAT, the BAT becomes hypertrophic and the WAT has a BAT-like phenotype. Their WAT expressed UCP1 and responded to β3-adrenergic stimulation, and the mice had a lower percent body fat and gained less weight on a high fat diet compared to wild-type mice. Another transgenic mouse, the RIP140-null mouse, was studied by Leonardsson et al. (2004) and found to have UCP1 expression in WAT, and these mice also had low percent body fat and resistance to obesity.

Seale et al. (2011) used an adenovirus that expressed shRNA to knock down PRDM16 in white adipocytes after induction of brown adipogenesis, leading to decreased BAT-specific gene expression and supporting the role of PRDM16 in brown adipogenesis. Tiraby and colleagues (2003) infected primary human white adipocytes with a PGC-1α adenovirus and saw increased UCP1 expression, which was enhanced with treatment with rosiglitazone (PPARγ agonist). Although these cells only expressed about 1% of the relative amount of UCP1 protein present in mouse brown adipocytes, they had increased oxidation of fatty acids, which the authors assert is the first evidence that human white adipocytes can increase oxidation of fatty acids.

Other attempts to create BAT

Kajimura and colleagues (2009) created brown adipocytes from human and murine skin fibroblasts by transducing them with retrovirus containing PRDM16 and C/EBPβ and then culturing them in adipogenic medium. After a week, the fibroblasts contained lipid, expressed UCP1 and PGC-1α. These cells had higher basal oxygen consumption than immortalized brown adipocytes but were unable to increase their respiration. The engineered brown adipocytes were transplanted into nude mice and grew into an ectopic BAT-like fat pad.

Schulz et al. (2011) treated progenitor cells from murine BAT, WAT, and skeletal muscle with BMP7 and found that 3 days of treatment prior to adipogenic differentiation could promote brown adipogenesis. However, the various progenitor cells exhibited different capacities for brown adipogenesis, with epididymal WAT being the least inducible. They transplanted the BMP7-treated cells into mouse muscle and saw development of an

ectopic brown fat depot. However, preadipocytes that were not treated with BMP7 did not differentiate well after transplantation. Human preadipocytes were also treated with BMP7 but needed it to remain in the medium in order to continue brown adipogenic differentiation. Further, they noted that preadipocytes from subcutaneous human WAT demonstrated better brown adipogenesis than cells from visceral fat depots.

In an interesting study in 2013, Stanford and colleagues transplanted BAT from donor mice to matched recipient mice. The recipients experienced improvements in metabolic parameters like insulin sensitivity and glucose tolerance, so dramatic as to reverse insulin resistance acquired from a high-fat diet. This study proved the principle that increased BAT mass in non-transgenic mice can positively impact metabolic homeostasis.

In vitro *measurement of cell respiration*

Beyond expression of UCP1 protein, the definition characteristic of brown adipose is its ability to uncouple oxidative phosphorylation from ATP synthesis. Therefore, it is important to know whether proported brown adipocytes differentiated in a lab actually function as expected. Researchers can measure respiration of animals, tissue, and cells in various ways, although many articles describing brown adipogenesis do not measure function of the differentiated cells. Techniques of measuring oxygen consumption have evolved. Kopecky et al. (1996) performed respirometry on pieces of tissue using a Warburg vessel, and one can determine energy expenditure of animals by housing them in metabolic chambers that measure oxygen consumption and carbon dioxide production (Seale et al., 2011). A Clark-type electrode has often been used to measure oxygen consumption of cells (Seale et al., 2011), but in more recent years, the Seahorse XF

Analyzer has been gaining popularity. Fewer cells are required for an XF assay, the cells can be adherent, it has higher throughput, and the results are comparable to those from a Clark electrode (Divakaruni et al., 2014).

Brief adipogenic differentiation time

Of note is the variety of methods for adipogenic differentiation with no standard regarding the medium used, time allotted for differentiation, or characteristics to define "mature" cells. The differentiation time varies widely, and ASCs from primary sources are often differentiated longer than immortalized cells. Hauner et al. (1989) differentiated primary progenitor cells for eighteen days, Smih et al. (2002) differentiated them for ten days, and in the hands of Tiraby et al. (2003), they were differentiated for thirteen days.

Even in the same lab there is inconsistency in the adipogenic protocol. The Spiegelman lab used immortalized and primary cells (Seale et al., 2008, 2011; Cohen et al;. 2014), which they cultured for two days in differentiation induction medium. They then switched to a differentiation medium with fewer drugs and used the cells for some experiments anywhere between day four and day eight of differentiation, although the day of use was not stated for all assays. Oxygen consumption was measured in primary cells using a Clark electrode after eight days of differentiation (2011). However, in the group's 2010 paper (Schulz et al.) they induced adipogenesis in progenitor cells for two days, switched to a different differentiation medium for another seven days, and used the cells for some experiments at day twelve. They measured expression of certain genes at days three, five, and twelve, and although the levels were continuing to increase, they did

not continue differentiation beyond day twelve. Also, they measured the cells' mitochondrial respiration with the Seahorse XF Analyzer after only the two days of induction.

Seahorse XF Analyzer

How it works

The Seahorse XF24 Analyzer uses proprietary 24-well cell culture microplates and assay cartridges. Probes on the cartridge correspond to the wells, and each probe has a sensor that detects oxygen dissolved in the medium. During an assay, the probe is lowered such that a microchamber is created above the cells, and oxygen consumption is measured for several minutes to calculate an oxygen consumption rate (OCR). The cartridges also have four drug delivery ports, and compounds can be added to the assay sequentially or in combination (Agilent Technologies, 2016). The OCR corresponds to mitochondrial respiration, and adding particular mitochondrial toxins to the assay allows one to elucidate the contribution to OCR from various mitochondrial proteins. After the assay, the data must be normalized to cell number.

Other methods for measuring mitochondrial respiration can require cell permeabilization or mitochondrial isolation, but the Seahorse XF Analyzer assays are conducted on live cells via a non-destructive process. Plates of cells can be reanalyzed and remain viable as long as no mitochondrial toxins are added. Other labs have measured respiration of

pieces of tissue with a Clark electrode and normalized to tissue weight (Cohen et al., 2014), but considering WAT and BAT vary in their structure and lipid content, we calculate OCR per cell by measuring DNA content.

Drugs and their effects on the mitochondria

To examine mitochondrial function during an XF assay, we administer oligomycin, FCCP, antimycin A, and rotenone to cells. Oligomycin A inhibits the F0 subunit of ATP synthase, stopping movement of protons from the intermembrane space to the matrix and conversion of ADP to ATP. The residual flow of protons out of the intermembrane space is called the proton leak, which occurs at baseline and be significant with activation of UCP1 (Jastroch et al., 2010). The decrease in OCR with addition of oligomycin A reflects the coupling efficiency, or the degree to which substrate oxidation and creation of the electrochemical gradient are connected, or "coupled" to ATP synthesis. Carbonyl cyanide-4-(trifluoromethoxy)phenylhydrazone (FCCP) dissipates the electrochemical gradient by carrying hydrogen ions across the mitochondrial inner membrane, thus acting as a chemical uncoupler (To et al., 2010). Addition of FCCP stimulates maximal respiration.

Antimycin A is a toxin produced by a bacterium, and it binds to Complex III and blocks oxidation of ubiquinol, inhibiting transport of electrons and maintenance of the electrochemical gradient (Ma et al., 2011). Rotenone is a pesticide that blocks electron transfer from Complex I to ubiquinone, inhibiting maintenance of the electrochemical gradient (Freestone et al., 2009). Injection of rotenone and antimycin A inhibit upstream

complexes of the electron transport chain, and the remaining measured respiration is non-mitochondrial. One should see a decrease in the oxygen consumption rate (due to impaired mitochondrial function) and an increase in glycolysis (further compensation for decreased mitochondrial ATP production). The non-mitochondrial respiration is subtracted from the raw OCR data to calculate the mitochondrial respiration.

Expectations for BAT and WAT

The basal respiration rates (oxygen consumption rate) for WAT and BAT should be different, with a higher respiration rate in BAT. Further, over 50% of BAT respiration is expected to be uncoupled from ATP synthesis. Addition of oligomycin eliminates the portion of the basal respiration that is due to ATP synthase activity (the portion of the proton gradient used by ATP synthase), so the residual respiration is due to protons "leaking" across the inner mitochondrial membrane. This allows measurement of coupling efficiency, which should be lower in BAT compared to WAT (due to presence of UCP1 in BAT).

FCCP carries protons across the mitochondrial inner membrane, effectively uncoupling the electron transport chain from ATP synthesis. Addition of FCCP "accelerates" the electron transport chain and allows us to measure maximal respiration and thus calculate the spare respiratory capacity. BAT is already "uncoupled" by UCP1, so the spare respiratory capacity may be lower in BAT compared to WAT. FCCP injection should also cause an increase in glycolysis (measured via extracellular acidification rate) as a way to compensate for the decreased ATP production from oxidative phosphorylation.

Goals of my project

Increased length of adipogenesis

As discussed above, there is not a standard time of adipogenesis, with groups running assays anywhere between two and eighteen days after induction of differentiation. Schulz et al. (2010) saw changes in gene expression over time, but did not continue the measurements beyond day twelve, despite lack of a plateau. In our hands, we have seen continued changes over a month, which is shown in our results, and past work in our lab has continued white adipogenesis of embryoid body-derived cells in 3D culture for six weeks (Hillel et al., 2009).

Use primary cells, not immortalized cells or viral vectors

We have a particular interest in translational research, so we desire to avoid using immortalized cells or viral vectors, as they are less immediately translatable to human medicine than use of primary cells. Further, Timmons et al. (2007) showed that primary white and brown preadipocytes have a different transcriptional profile than immortalized white or brown preadipocytes. Kajmura et al. (2009) saw different respiratory profiles in their immortalized brown adipocytes compared to fibroblasts that had been differentiated into brown adipocytes via retroviral gene delivery. With these questions of what kind of lab-created brown adipocyte is closest to "real" BAT, and with our interest in translational research, we decided to use ASCs harvested from primary tissue.

Fill gap in knowledge regarding respiration of primary cell-derived ASCs and adipocytes

We compare mitochondrial respiration of white and brown ASCs, as well as that of fully differentiated rat and human ASCs that have undergone brown and white adipogenesis. To our knowledge, the gene expression profiles and mitochondrial respiration of these differentiating, non-immortalized, non-transfected cells have not previously been examined out to four weeks.

Fill gap in tissue engineering regarding study of BAT

As discussed, many researchers are using transgenic mice or viruses to study regulation of BAT and explore ways to enhance energy expenditure from both BAT and WAT. However, there is a lack of overlap between tissue engineering and BAT fields. The work on BAT has been exclusively in cells grown in monolayer or in animals. However, conducting experiments with cells grown in a 3D environment, mimicking their natural conformation, is an important step on the road to discovery.

Our lab has experience with harvesting adipose-derived stem cells, and we have created implants composed of synthetic scaffolds seeded with ASCs that have been differentiated into a variety of mature cell types. We now have applied our experience and expertise to create synthetic brown adipose "tissue." While other attempts in the field to "engineer" BAT have focused on genetic engineering, such as using viral vectors or genetically modified mice, our technique uses a combination of drugs and environment to

differentiate adipose-derived stem cells to brown adipocytes in a 3-dimensional synthetic scaffold. Further, we have been able to measure oxygen consumption per cell in our engineered WAT and BAT, which informs the literature regarding differences between rat versus human cells and 2D versus 3D environments. Here we show that the physiologic and mechanical environments influence brown adipogenesis, impacting differentiation lineage and function of mature cells.

MATERIALS AND METHODS

Cell Isolation.

Interscapular brown adipose tissue (BAT) and inguinal white adipose tissue (WAT) were harvested from adult Sprague-Dawley rats, and human subcutaneous WAT was harvested from abdominoplasty surgical waste from the University of Maryland. To isolate ASCs the tissue was digested with 0.1% collagenase type I (Worthington) at 37°C for 2 hours, then centrifuged, and the top layer of oil and floating adipocytes were removed. Erythrocytes were lysed with a solution of 155 mM NH_4Cl, 10 mM $KHCO_3$, and 0.1 mM EDTA, adjusted to pH 7.3, and the slurry was passed through a 40 um cell strainer and centrifuged. The cell pellet was resuspended in DMEM/F12 (Gibco (Life Technologies), Grand Island, NY, USA) supplemented with 10% fetal bovine serum (FBS; Thermo Fisher Scientific, Waltham, MA, USA) and 100 U/mL penicillin and 100

μg/mL streptomycin (Pen Strep; Gibco), plated in tissue culture flasks, and cultured at 37°C in 5% CO_2. Human ASCs were expanded in growth medium supplemented with 8 ng/mL bFGF (Peprotech, Rocky Hill, NJ, USA). The cells were expanded and at passage 4 they were plated at 5000 cells/cm^2 and cultured in brown or white adipogenic media after reaching ~80% confluency.

Migration study

Brown or white ASCs were starved of serum for 24 hours prior to being seeded in the upper chamber of 6.5 mm transwells (Sigma-Aldrich, St. Louis, MO, USA) at 25,000 cells/well. To the bottom of the wells was added 10% FBS (positive control), serum-free medium (negative control, or ECM from brown or white adipose in low or high concentrations (1 or 10 μg/mL). The process for preparation of adipose ECM is described in Wu et al. (2012). Three transwells were tested per condition. After 6 hours, cells from the upper side of the membrane were removed and cover slips were mounted on the bottom of the membrane with Vectashield with DAPI (Fisher Scientific, Pittsburgh, PA, USA). Three images were taken per well, and cells were counted from the images using ImageJ software.

Cell differentiation

To differentiate ASCs to white adipocytes, we cultured them in adipogenic medium composed of high-glucose (25 mM) DMEM (Gibco) supplemented with 10% FBS, 100

U/mL penicillin and 100 μg/mL streptomycin, 1 μM dexamethasone (Sigma-Aldrich), 100 μM indomethacin (Sigma-Aldrich), 500 μM 3-isobutyl-1-methylxanthine (IBMX; Sigma-Aldrich), and 10 μg/mL bovine insulin (Cell Applications, San Diego, CA, USA). Brown adipogenic medium was composed of high glucose DMEM with 10% FBS, 100 U/mL penicillin and 100 μg/mL streptomycin, 0.5 μM dexamethasone, 125 nM indomethacin, 250 μM IBMX, 850 nM bovine insulin, 1 μM rosiglitazone (a PPARγ agonist) (Cayman Chemical Company, Ann Arbor, MI, USA), and triiodothyronine (T3, thyroid hormone; 1 nM for rat ASCs, 250 nM for human ASCs) (Sigma-Aldrich). ASCs from BAT and WAT were cultured in adipogenic media both in 2D monolayer and encapsulated in 3D hydrogels. The media were changed three times per week.

Hydrogel encapsulation and 3D culture

Hydrogels were formed with UV-sterilized poly(ethylene glycol)-diacrylate (PEGDA; SunBio, Anyang City, South Korea) at either 5% or 10% w/v in sterile PBS, with or without functionalization with RGD peptide (arginine-glycine-aspartate) in the form of CDYRGDS at 0.5% w/v. CD (cyclodextrin rings) were added to minimize the effect on the mechanical properties of the hydrogel (peptide conjugation previously described in Singh et al., 2013). The photoinitiator Irgacure 2959 (Ciba Specialty Chemicals (BASF Corp.), Florham Park, NJ, USA) was dissolved in 70% ethanol and added to the PEGDA solution at a final concentration of 0.5 mg/mL. ASCs were suspended in the hydrogel solution at 20 million cells/mL and pipetted into 20 uL or 100 uL molds. The gels were photopolymerized under UV light for 5 minutes, removed from the molds, and incubated

in 12-well non-tissue culture plates in white or brown adipogenic media at 37°C with 5% CO_2.

In vivo *study*

Rat ASCs derived from BAT were encapsulated in 100 uL 10% PEGDA hydrogels, differentiated *in vitro* in brown adipogenic medium for 4 weeks, and then implanted subcutaneously along the dorsum of athymic rats. The implants were harvested at 1 month after implantation. Immunohistochemistry was performed on the samples, probing for UCP1 and PPARγ, and samples were stained with Alizarin Red to show the presence of calcium.

Cell staining and histology

Monolayer cells were fixed with 10% formalin for 10 minutes, and hydrogels were cut in half and fixed in 10% formalin overnight. The hydrogels were embedded in paraffin after a standard histological dehydration protocol, and 5 um sections were prepared. Cells in monolayer were stained with 3 mg/mL Oil Red O in 50.4% triethyl phosphate to assess lipid content. To evaluate calcification in hydrogels, sections were stained with 1% Alizarin Red S solution at pH of 4.1 – 4.3 for 5 minutes. Immunocytochemistry (ICC) and immunohistochemistry (IHC) were performed using antibodies against UCP1 (1:500, rabbit anti-UCP1; Abcam, Cambridge, MA, USA) and PPARγ (1:50, rabbit anti-PPARγ; Santa Cruz Biotechnology, Santa Cruz, CA, USA) for a qualitative assessment of

expression of those proteins. For ICC the primary antibody was detected with Alexa Fluor 594 goat anti-rabbit (Life Technologies) and nuclei were stained with 0.1 μg/mL Hoechst 33342 (Invitrogen), and for IHC the primary antibody was detected with the SuperPicTure HRP Polymer Conjugate Rabbit Primary (DAB) KIT (Invitrogen). Images of monolayer cells were taken using a Zeiss Axio Observer.A1 inverted microscope (Carl Zeiss Microscopy, Thornwood, NY, USA) with a 40x objective, and images of cells in hydrogels were obtained with a Zeiss Axio Imager.A2 upright microscope (Carl Zeiss Microscopy) with a 40x objective.

Real time quantitative PCR

Expression of adipose-specific genes (Adiponectin, FABP4, PPARγ), and BAT-specific genes (UCP1, PRDM16, PGC-1α, Cidea) was quantified using real time quantitative PCR. RNA was isolated from cells using TRIzol (Life Technologies), SuperScript III Reverse Transcriptase (Life Technologies) was used to synthesize cDNA, and SYBR Green (Life Technologies) was used for dsDNA detection. Each PCR reaction was performed in triplicate, and the fold change in expression of the genes is presented as $2^{-\Delta\Delta CT}$ where β-actin was used as the endogenous reference, and the change is relative to expression of undifferentiated ASCs unless otherwise noted.

Metabolic analysis

We used the Seahorse Biosciences XF24 Extracellular Flux Analyzer to assess the metabolic function of live cells. The XF Analyzer measures the oxygen consumption rate (OCR) and extracellular acidification rate (ECAR) of live cells in real time by creating a 7 uL microchamber around monolayer cells and measuring the oxygen in and pH of the medium using fluorescent probes. After four weeks of differentiation, cells were plated at a density of 20,000 cells/well on 24-well XF microplates (Seahorse Bioscience, Billerica, MA, USA) coated with 0.1% gelatin. Assays were conducted 1 week after plating. Cells encapsulated in 5% PEGDA hydrogels were assessed 5 weeks after initiation of differentiation, and the XF islet capture plates were used. Unbuffered white or brown XF assay media were prepared on the day of each assay, using XF assay medium (Seahorse Bioscience) supplemented with 1 mM sodium pyruvate, 25 mM glucose, and the respective concentrations of drugs found in the differentiation media. The media were warmed to 37°C, brought to pH 7.4, and filter-sterilized. The cells were rinsed three times with XF medium and put in a 37°C incubator without CO_2 for 45 minutes prior to the assay. The oligomycin, FCCP, rotenone, and antimycin A were dissolved at 10x concentration in XF medium such that the final working concentrations for the compounds were: 1 μM oligomycin; 250 nM FCCP for monolayer cells, 10 μM FCCP for hydrogels; 2 μM rotenone; 2 μM antimycin A. These compounds were purchased from Seahorse Bioscience. The drugs were loaded into the injection ports of the XF cartridge for the assay, and after at least four basal measurements, oligomycin, FCCP, rotenone, and antimycin A were injected sequentially to characterize the mitochondrial function of the cells. At least four measurements were taken after injection of each drug. The changes in OCR after treatment with these compounds allow

us to determine the basal mitochondrial respiration, the amount of proton leak, and the spare respiratory capacity of the cells. At the end of each assay, cells were rinsed with PBS and lysed with cold lysing solution (10 mM Tris, 1 mM EDTA, 0.1% Triton X-100, 0.1 mg/mL proteinase K), and the lysates were transferred to microcentrifuge tubes. Hydrogels were frozen with liquid nitrogen and homogenized with pestles in individual microcentrifuge tubes before adding lysing solution. The lysates were digested overnight at 50°C. To normalize the metabolic data, the PicoGreen DNA assay was performed on the lysate from each XF well to measure the DNA content of the cells.

Results are presented as the mean +/- SD. The t-test and one-way ANOVA with Tukey's post-test were used to determine differences between groups, as appropriate. A p-value of < 0.05 was considered statistically significant. Statistical analyses were performed with GraphPad Prizm 5 software.

RESULTS

Comparison of rat white and brown ASCs

As shown in Figure 1A and 1B, the migration responses of rat brown and white adipose-derived stem cells to ECM derived from rat brown and white adipose were analyzed. The positive control was 10% FBS, serum-free medium served as a negative control, and low

and high concentrations (1 or 10 μg/mL) of brown or white adipose ECM were the tested conditions. In Figure 1A, the results are grouped by brown or white ASCs to show their responses to ECM by cell type. Among ECM types, the brown ASCs were most attracted to the high concentration of white adipose ECM, although the low concentration also induced migration significantly. Their migration response to BAT ECM was significantly different than serum-free medium only at the lower concentration of ECM. The white ASCs only had a significant migration response to the low concentration of BAT ECM and the high concentration of WAT ECM. Figure 1B groups the results by type of stimulus and compares the responses of brown and white ASCs to each other. The brown ASCs migrated significantly more toward the 10% FBS, the low concentration of BAT ECM, and both concentrations of WAT ECM. However, their basal migration rate is the same, as there is no difference in their response to serum-free medium. Neither cell type migrated toward the high concentration of BAT ECM.

The basal gene expression of rat brown and white ASCs was compared after one day in growth medium and is represented as fold change relative to gene expression of the white ASCs (Figure 2). Adipose-specific genes were evaluated in order to establish a baseline prior to differentiation. The brown ASCs had less basal expression of the fat genes adiponectin, PPARγ, and FABP4, and they had greater expression of the brown fat gene UCP1.

The ASCs were further characterized by measuring their basal mitochondrial respiration (Figure 3) before differentiation. The basal mitochondrial respiration is calculated by subtracting the non-mitochondrial respiration from the initial measurements of OCR, before any drugs are applied to the assay. OCR per cell was significantly higher in

brown ASCs than in white ASCs, further confirming the fact that these cells have different functions.

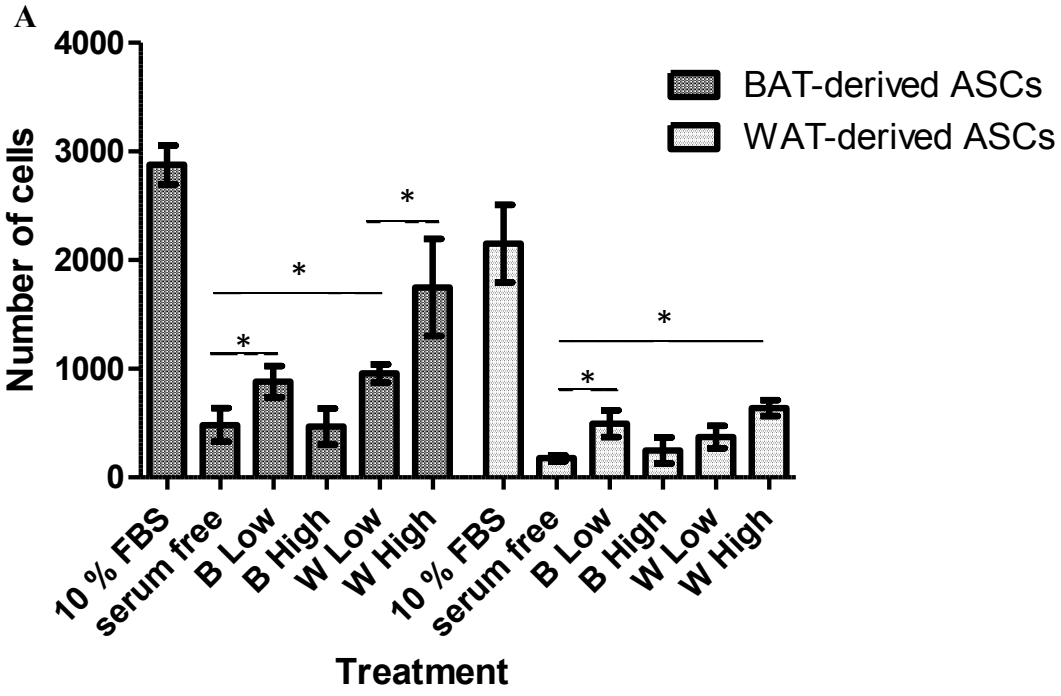

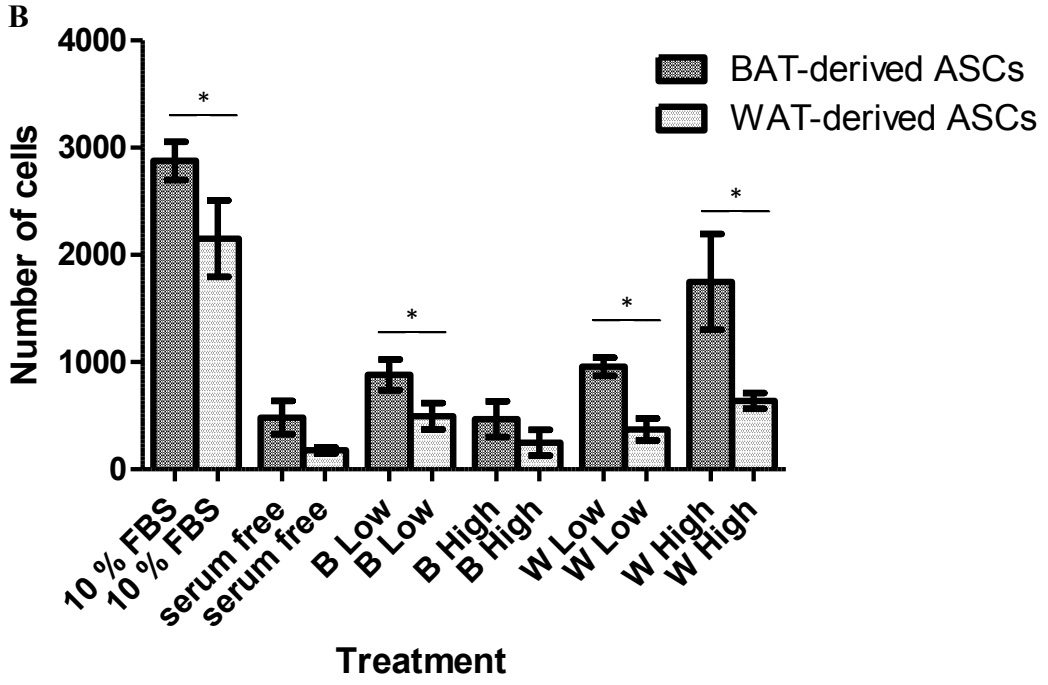

Figure 1. ASC migration response to ECM, organized by cell type (A) or by stimulus (B). Brown and white ASCs migrated across transwells in response to ECM from brown or white adipose at low or high concentrations. B = BAT-derived ECM; W = WAT-derived ECM; Low = 1 μg/mL; High = 10 μg/mL. * : $p < 0.05$.

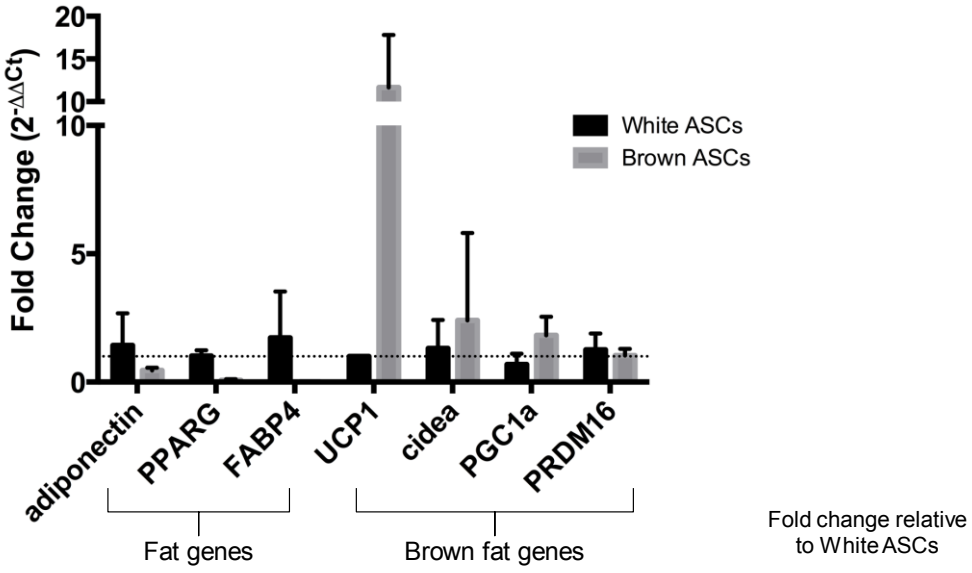

Figure 2: Gene expression of undifferentiated rat ASCs. The basal gene expression of rat brown and white ASCs is represented as fold change relative to gene expression of rat white ASCs.

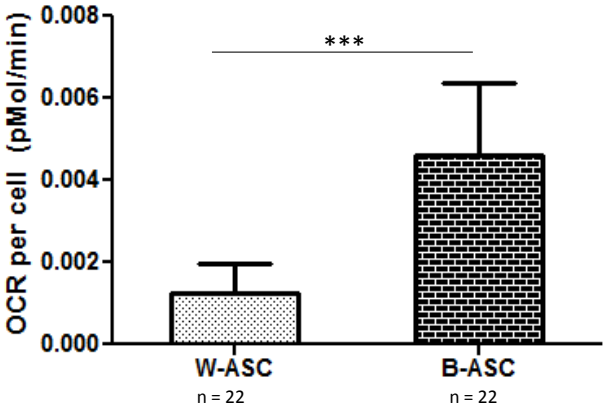

Figure 3: The basal mitochondrial respiration of rat adipose-derived stem cells, shown as oxygen consumption rate per cell. *** = $p < 0.001$.

Adipogenic differentiation of ASCs in monolayer

Using white and brown adipogenic media, rat white ASCs and brown ASCs were differentiated for four weeks to white and brown adipocytes, respectively. White ASCs were also differentiated to brown adipocytes. Their phenotypes were characterized with immunocytochemistry to identify expression of UCP1 and PPARγ proteins and with Oil Red O staining to evaluate lipid content (Figure 4). Hoechst stain was used to identify nuclei. The differentiated cells contained lipid (left column, red) and were immunoreactive for PPARγ (center column, green), and the brown adipocytes were also immunoreactive for UCP1 (right column, green). Further, the "white-to-brown" cells also showed UCP1 immunoreactivity, appearing to have the same phenotype as the brown adipocytes. As expected, the white adipocytes did not express UCP1.

The same differentiation procedure was completed on ASCs from human subcutaneous white adipose tissue, with white ASCs undergoing white and brown adipogenesis for four weeks (Figure 5). Both white and brown differentiated adipocytes were full of lipid (left column, red) and expressed PPARγ (center column, green). Although the white ASCs that differentiated to brown adipocytes were immunoreactive for UCP1, surprisingly some of the white adipocytes also expressed UCP1 (right column, green).

Beyond evaluating cells at the end of differentiation, gene expression of ASCs undergoing adipogenesis was measured with RT-PCR weekly across the 28-day differentiation period. Genes of interest included adipose-specific adiponectin, PPARγ,

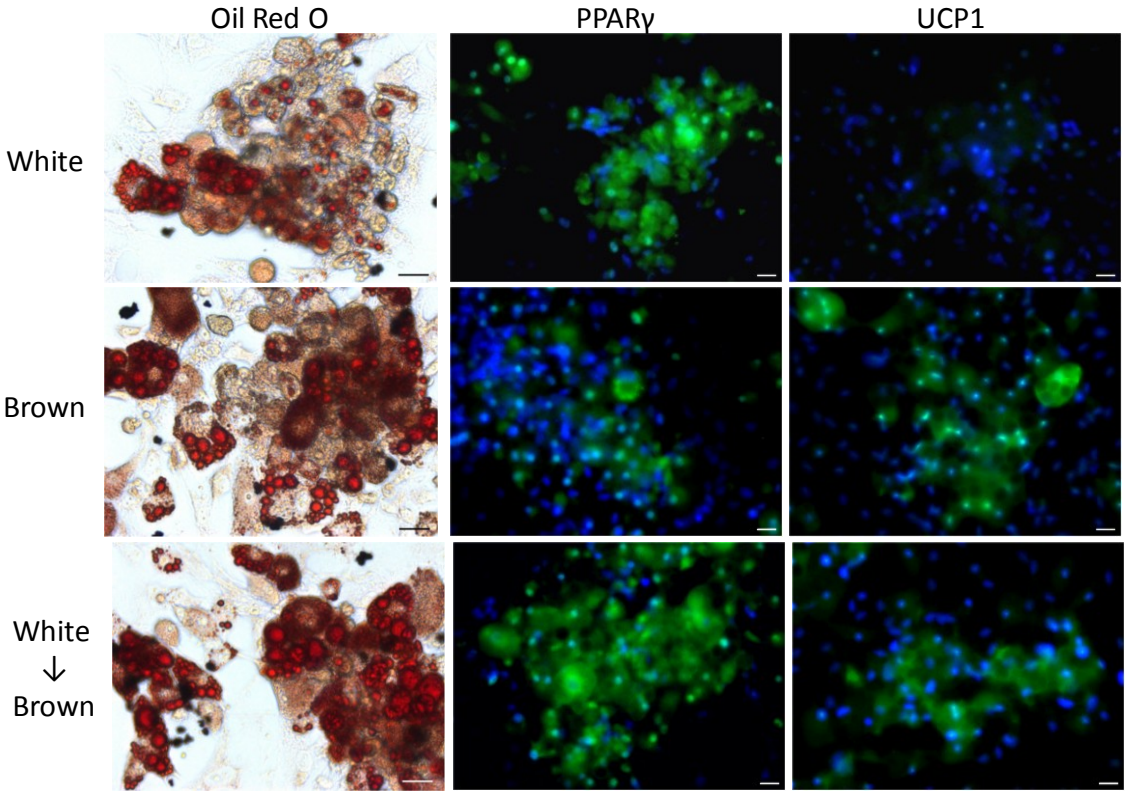

Figure 4: Adipogenic differentiation of rat ASCs, four weeks. Oil Red O reveals lipid droplets in cells. Immunostaining confirms presence of PPARγ (center, green) and UCP1 (right, green). Nuclei are blue in fluorescent images. "White" = white adipogenic differentiation of white adipose-derived stem cells. "Brown" = brown adipogenic differentiation of brown adipose-derived stem cells. "White → Brown" = brown adipogenic differentiation of white adipose-derived stem cells. Scale bar = 20 μm.

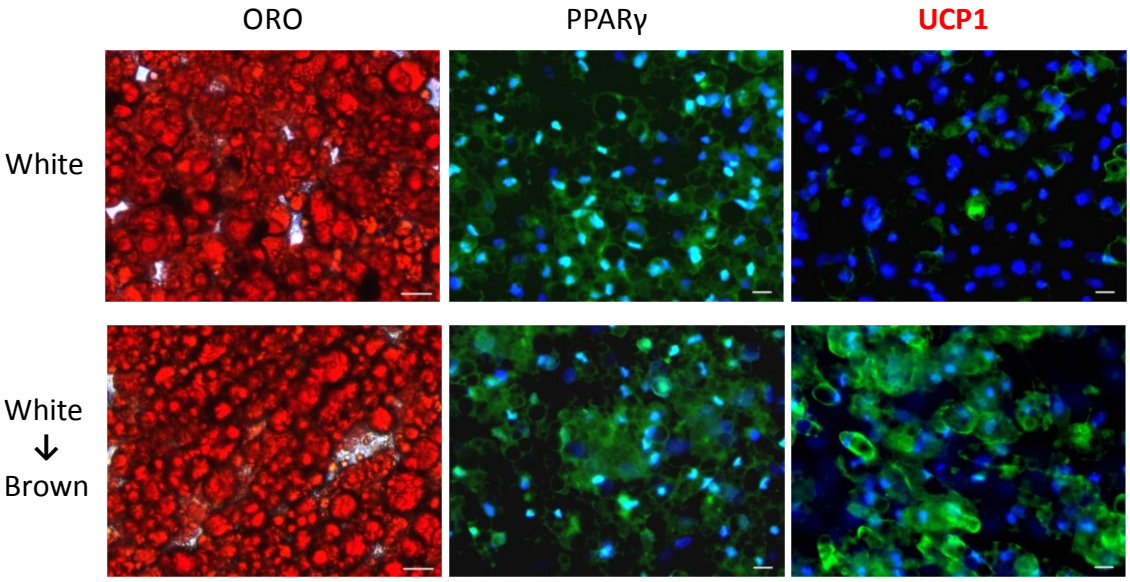

Figure 5: Adipogenic differentiation of human ASCs, four weeks. Oil Red O shows lipid-laden cells. Immunostaining confirms presence of PPARγ (center, green) and UCP1 (right, green). Nuclei are blue in fluorescent images. "White" = white adipogenic differentiation of white adipose-derived stem cells. "White → Brown" = brown adipogenic differentiation of white adipose-derived stem cells. Scale bar = 20 μm.

FABP4, and brown adipose-specific UCP1, cidea, and PGC-1α. Figure 6A shows results from rat white ASCs and brown ASCs undergoing white and brown adipogenesis, respectively, and Figure 6B is data from rat white ASCs differentiating to brown adipocytes ("white-to-brown" adipocytes). RT-PCR analysis of RNA taken weekly over four weeks of adipogenesis demonstrated increases in adipose-specific genes, represented as fold change relative to basal "Day 0" gene expression of rat white adipose-derived stem cells. Both white and brown adipocytes showed increased expression of adipose-specific genes (adiponectin, PPARγ, FABP4), and the brown adipocytes had greater

expression of brown-adipose specific genes (UCP1, cidea, PGC-1α) than the white adipocytes. The white-to-brown adipocytes also showed increased expression of adipose-specific genes (adiponectin, PPARγ, FABP4) and brown-adipose specific genes (UCP1, Cidea, PGC-1α), with the greatest fold change in PGC-1α expression among the brown-adipose specific genes. Their expression of adipose-specific genes was comparable to that of white adipocytes, and their expression of brown adipose-specific genes was similar to that of white adipocytes until days 21 and 28, when the expression began to increase, although not reaching the level of brown adipocytes.

The gene expression of human white ASCs undergoing white or brown adipogenesis was also evaluated over 28 days (Figure 7), looking at the same genes as examined in the rat ASCs, in addition to the brown adipose-specific PRDM16. RT-PCR analysis of RNA taken weekly over four weeks of adipogenesis demonstrated increases in gene expression, represented as fold change relative to basal "Day 3" gene expression of human white ASCs. The upper two graphs show changes in adipose-specific genes and the lower two graphs show changes in brown adipose-specific genes.

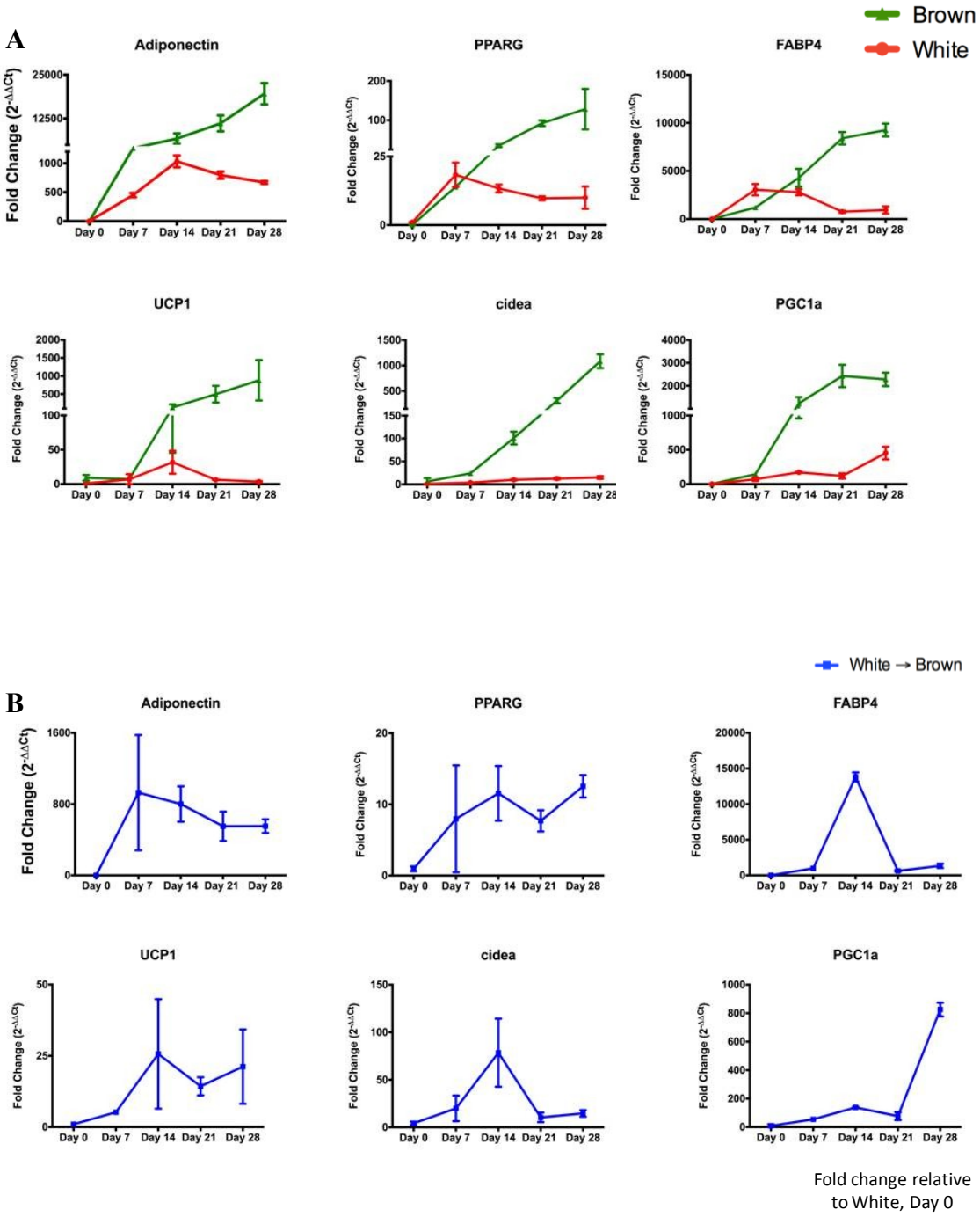

Figure 6: Changes in gene expression with adipogenesis of rat ASCs across four weeks. This figure represents changes in gene expression of rat white ASCs and brown ASCs undergoing white and brown adipogenesis, respectively (A) and of white ASCs undergoing brown adipogenesis (B). RT-PCR analysis of RNA taken weekly over four weeks of adipogenesis demonstrated increases in adipose-specific genes. Data is represented as fold change relative to basal "Day 0" gene expression of rat white adipose-derived stem cells. "Brown" (green line) = brown adipogenesis of brown ASCs. "White" (red line) = white adipogenesis of white ASCs. "White → Brown" (blue line) = brown adipogenesis of white ASCs.

Both white adipocytes and white-to-brown adipocytes showed increased expression of adipose-specific genes (adiponectin, PPARγ, FABP4), which plateaued or decreased after the first week of differentiation. Interestingly, human ASCs showed increased expression of the brown adipose-specific genes UCP1 and cidea whether they were undergoing white or brown adipogenesis, which is reminiscent of the UCP1 immunoreactivity of white and brown adipocytes (shown in Figure 5). Neither white adipocytes nor

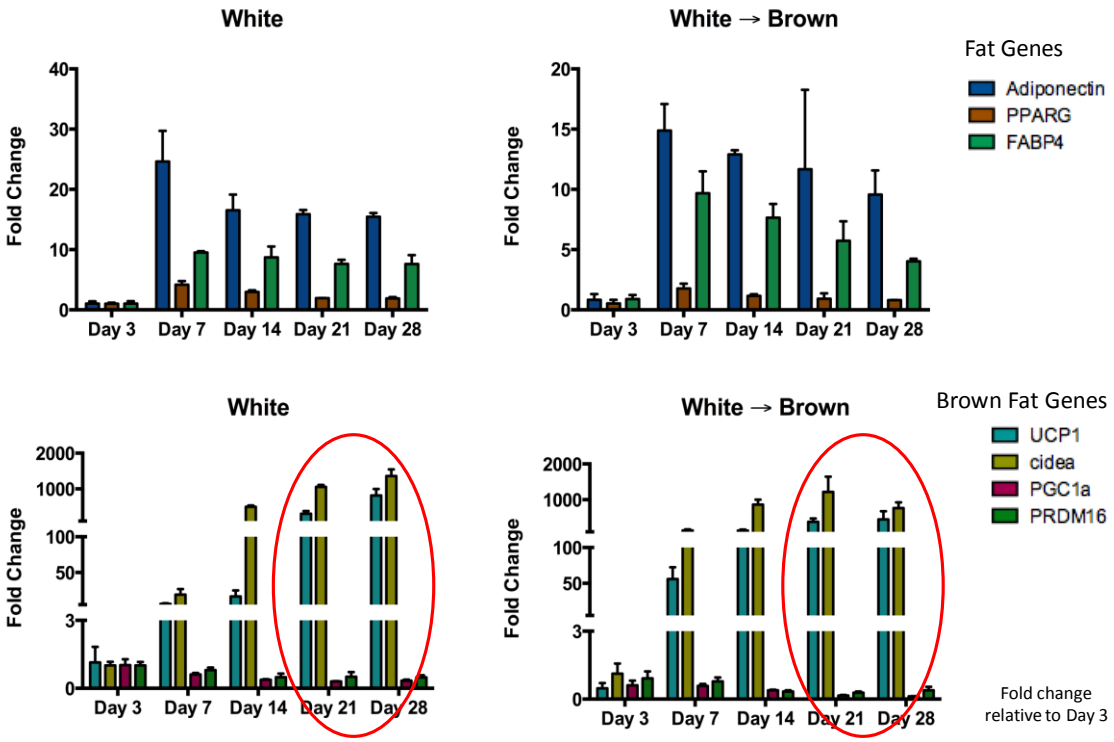

Figure 7: Changes in gene expression with adipogenesis of human ASCs across four weeks. This figure represents changes in gene expression of human white adipose-derived stem cells undergoing white or brown adipogenesis. The upper two graphs show changes in adipose-specific genes and the lower two graphs show changes in brown adipose-specific genes. RT-PCR analysis of RNA taken weekly over four weeks of adipogenesis demonstrated increases in gene expression, represented as fold change relative to basal "Day 3" gene expression of human white ASCs. "White" = white adipogenic differentiation of white adipose-derived stem cells. "White → Brown" = brown adipogenic differentiation of white adipose-derived stem cells.

white-to-brown adipocytes demonstrated increased expression of PGC-1α or PRDM16. Human ASCs undergoing brown adipogenesis expressed brown adipose-specific genes at higher levels sooner than human ASCs undergoing white adipogenesis, but by Day 21 the fold changes of UCP1 and Cidea were about the same in both groups (circled in red).

Beyond changes in gene expression, the function of the differentiated adipocytes was evaluated by assessing their mitochondrial respiratory profiles. It was expected that brown adipocytes would have higher basal respiration than white adipocytes, and it was hoped that the white-to-brown adipocytes would function like brown adipocytes. Figure 8A compares oxygen consumption rates (OCR) of ASCs to their respective differentiated cells, showing an increase of basal OCR with differentiation. Interestingly, the brown ASCs had higher respiration than the differentiated white adipocytes. As shown in Figure 8B, rat brown adipocytes had higher basal respiration than white adipocytes as expected. Surprisingly, the white-to-brown adipocytes had significantly higher basal respiration than both brown and white adipocytes, with a basal OCR about 4-fold higher than that of white adipocytes and about 2-fold higher than that of brown adipocytes. To examine uncoupling of the adipocytes, oligomycin was administered to inhibit the F_0 subunit of ATP synthase, and the OCR was measured. Figure 8C compares the OCR due to proton leak among the three types of differentiated adipocytes after 5 weeks of adipogenic differentiation. The proton leak represents the level of uncoupling of the cells, and this portion of mitochondrial respiration is calculated by subtracting the non-mitochondrial respiration from the post-oligomycin respiration. As expected, the level of uncoupling of brown adipocytes was higher than that of white adipocytes. Interestingly, the white-to-brown cells had significantly higher proton leak and were more uncoupled

A **Basal mitochondrial oxygen consumption rate**

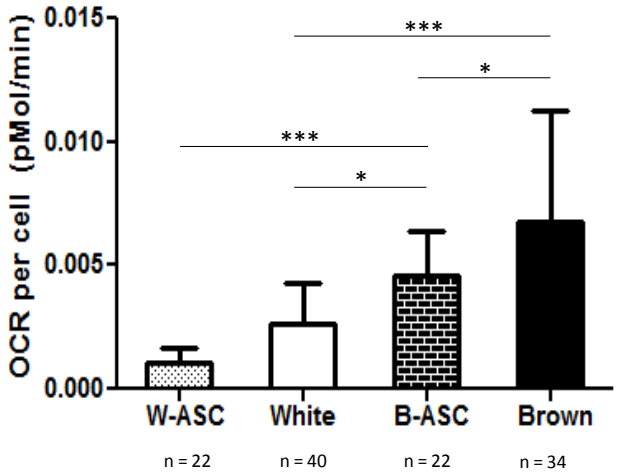

B **Basal mitochondrial oxygen consumption rate**

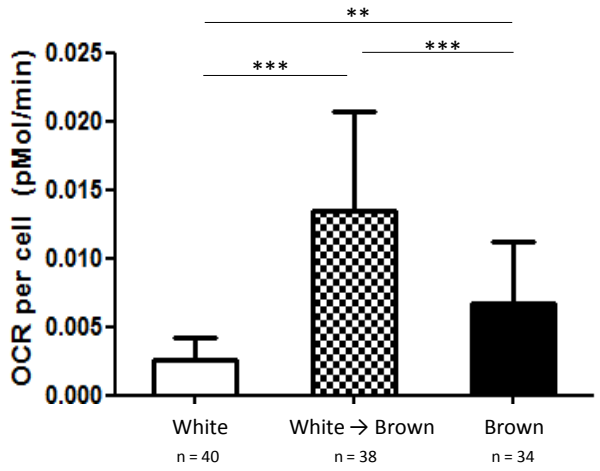

C **OCR Due to Proton Leak**

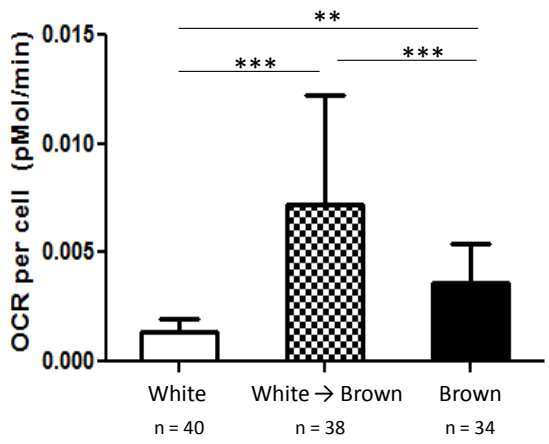

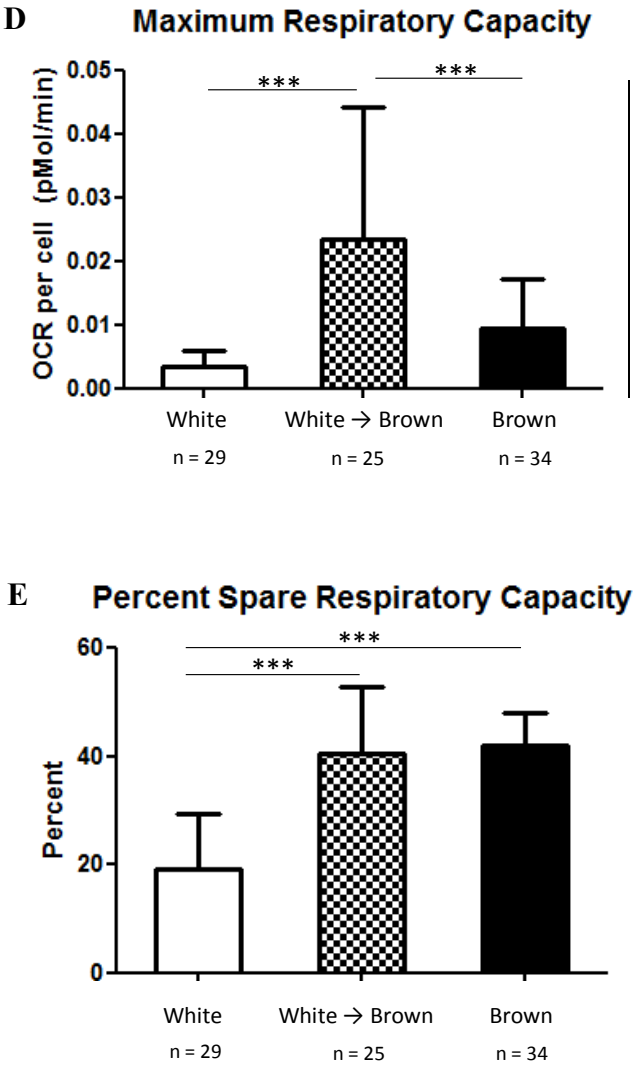

Figure 8: Mitochondrial respiratory profile after adipogenic differentiation of rat ASCs. **A**: Change in basal mitochondrial respiration of rat ASCs after adipogenic differentiation for 5 weeks. **B**: Comparison of basal mitochondrial respiration among the three types of differentiated adipocytes after 5 weeks of adipogenic differentiation. **C**: OCR due to proton leak among the three types of differentiated adipocytes. **D**: Comparison of the maximum respiratory capacity among the three types of differentiated adipocytes. **E**: Percent spare respiratory capacity, or the percent of maximum respiration that is reserved, among the three types of differentiated adipocytes. W-ASC = white adipose-derived stem cells. B-ASC = brown adipose-derived stem cells. "White" = white adipogenic differentiation of white ASCs. "White → Brown" = brown adipogenic differentiation of white ASCs. "Brown" = brown adipogenic differentiation of brown ASCs. * : $p < 0.05$; ** : $p < 0.01$; *** : $p < 0.001$.

than both white and brown adipocytes. To measure the maximum respiratory capacity of the adipocytes, the ionophore FCCP was added to the cells. The maximum respiratory capacity is calculated by subtracting the non-mitochondrial respiration from the respiration measured after addition of FCCP to the cells. Figure 8D compares the maximum respiratory capacity among the three types of differentiated adipocytes. The white-to-brown adipocytes had significantly higher maximum respiratory capacity than both white and brown adipocytes, while the maximum respiratory capacity did not differ significantly between white and brown adipocytes. The spare respiratory capacity is the difference between the basal OCR and the OCR after addition of FCCP. To calculate the percent spare respiratory capacity, or the percent of maximum respiration that is reserved, the spare respiratory capacity is divided by the maximum respiratory capacity and multiplied by 100. Figure 8E compares the percent spare respiratory capacity among the three types of differentiated adipocytes. Although the white-to-brown adipocytes had significantly higher maximum respiratory capacity than white and brown adipocytes (Figure 8D), their percent spare respiratory capacity was not significantly different from that of brown adipocytes. The percent spare respiratory capacity of white adipocytes was significantly lower than that of brown and white-to-brown adipocytes.

The mitochondrial profile of differentiated human ASCs was also assessed. Figure 9A demonstrates that the basal mitochondrial respiration increases with differentiation of human white ASCs to white adipocytes or to brown adipocytes. However, no significant difference in basal respiration was exhibited between white and white-to-brown adipocytes. Surprisingly, the white adipocytes had significantly higher proton leak (Figure 9B), meaning they were more uncoupled than the white-to-brown adipocytes,

even though both types of adipocytes showed UCP1 immunoreactivity (Figure 5). The maximum respiratory capacity did not differ significantly between white adipocytes and white-to-brown adipocytes, but the white adipocytes had significantly higher percent spare respiratory capacity than the white-to-brown adipocytes.

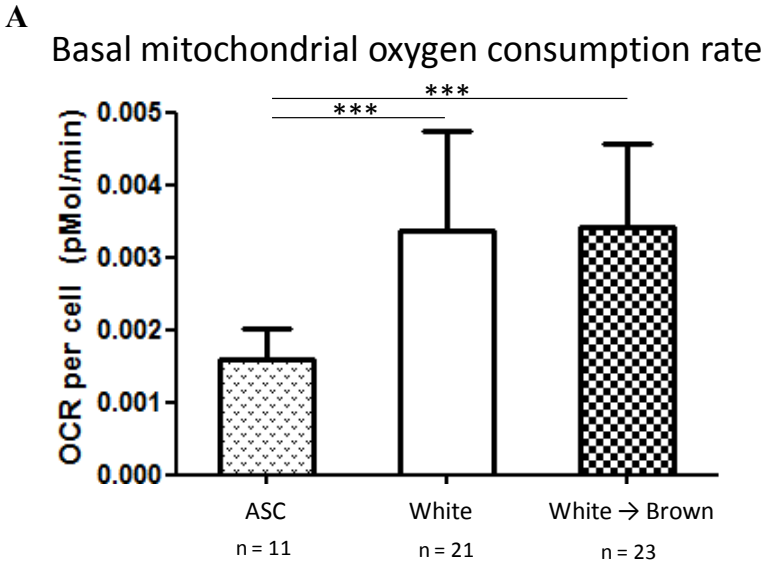

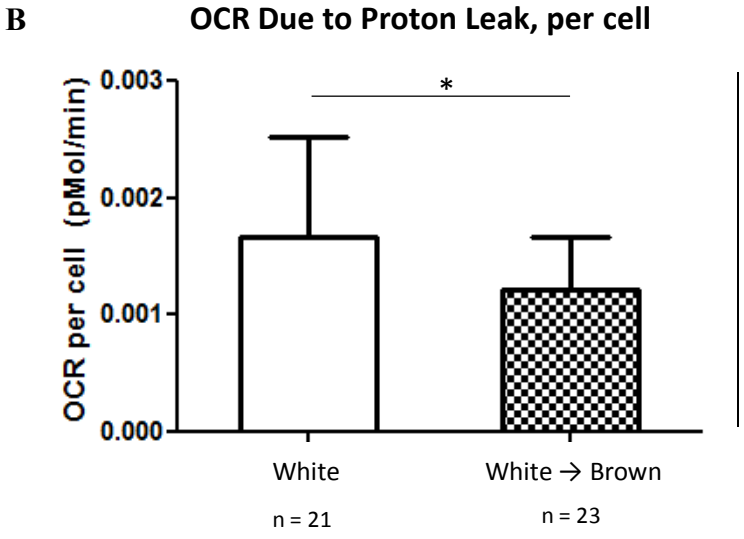

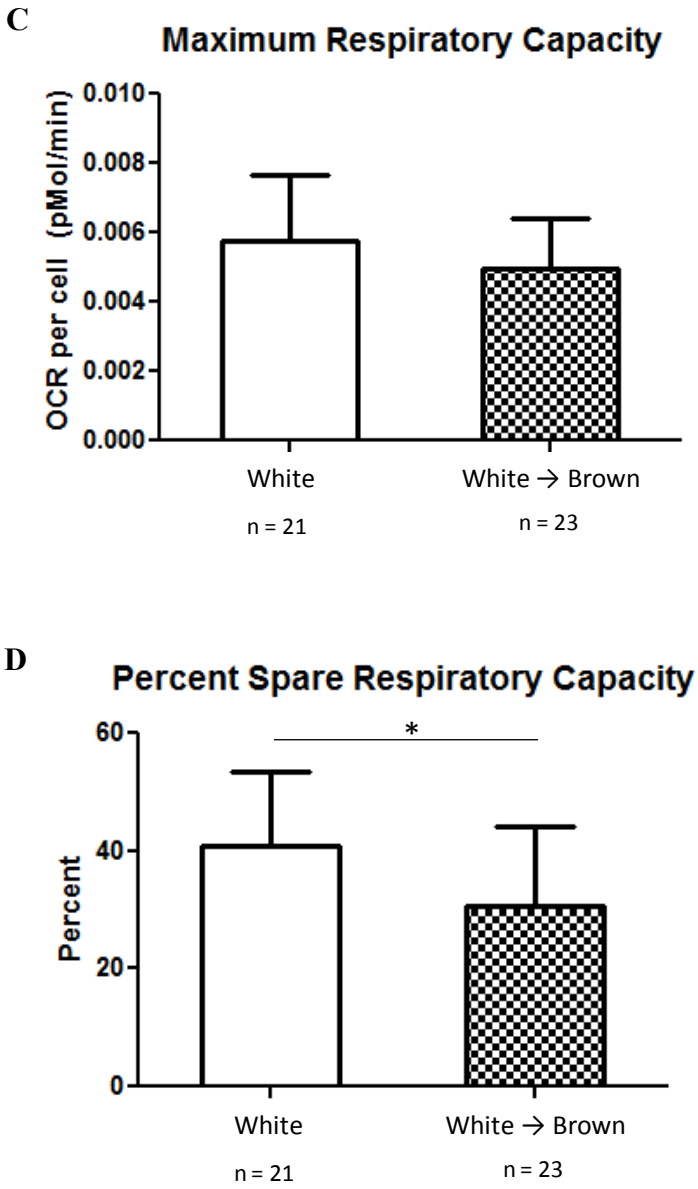

Figure 9: Mitochondrial respiratory profile after adipogenic differentiation of human ASCs. **A**: Change in basal mitochondrial respiration of human ASCs after adipogenic differentiation for 5 weeks. **B**: OCR due to proton leak between white and white-to-brown adipocytes. **C**: Comparison of the maximum respiratory capacity between the two types of differentiated adipocytes. **D**: Percent spare respiratory capacity, or the percent of maximum respiration that is reserved, between white and white-to-brown adipocytes. "ASC" = human white adipose-derived stem cells. "White" = white adipogenic differentiation of human white ASCs. "White → Brown" = brown adipogenic differentiation of human white ASCs. * : $p < 0.05$; *** : $p < 0.001$.

In vivo *differentiation of encapsulated rat ASCs*

As the author's lab had experience encapsulating cells in 10% PEG hydrogels and implanting them into rats, the next step of the present study was to assess *in vivo* differentiation of rat brown ASCs. The ASCs were encapsulated in 10% PEG hydrogels and cultured in brown adipogenic medium *in vitro* for four weeks prior to implantation in immunocompromised rats. Four weeks later, the constructs were removed and a dramatic effect of the local environment on differentiation was observed. When the implants were cut for processing, it was clear that the center had calcified. Sections were probed for immunoreactivity against UCP1 and PPARγ, as well as stained for calcium with Alizarin Red. The left image of Figure 10 is a cross-section of an implant stained with Alizarin Red and viewed at low magnification. The center of the construct is full of cells that have deposited calcium-rich ECM. The center and right images are taken at high magnification of cells at the periphery of the implant, and those cells show immunoreactivity for PPARγ and UCP1 respectively. Despite ASCs at the center of the implant undergoing osteogenesis, the cells at the edges of the constructs had

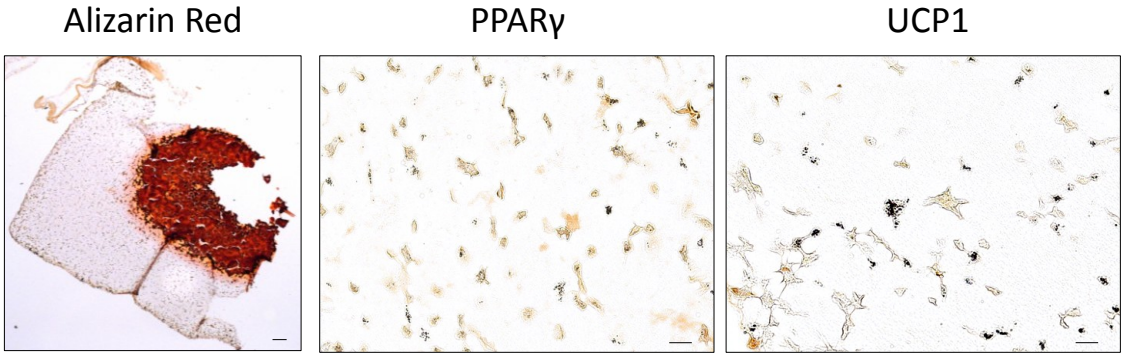

Figure 10. Effect of local environment on differentiation of brown ASCs. Left image, scale bar = 200 μm. Center and right images, scale bar = 20 μm.

characteristics of brown adipocytes. This figure shows a dramatic example of how the microenvironment within a hydrogel can influence differentiation, even in the presence of chemical cues steering differentiation in another direction.

Influence of the scaffold on adipogenic differentiation

Upon the observations from the *in vivo* experiment, the next step of the study was to optimize the hydrogel to support brown adipogenesis throughout the construct. ASCs were encapsulated in various scaffolds that had modified adhesion and stiffness, with a goal of delineating which environments encourage brown adipogenic differentiation. The size of the construct was also modified to improve diffusion of oxygen and nutrients to the center of the gel. Figure 11 evaluates the impact of matrix stiffness on brown adipogenesis of rat brown ASCs. Cells underwent 4 weeks of brown adipogenic differentiation in either 5% PEG gels (softer) or 10% PEG gels (stiffer). Sections of the hydrogels were probed for UCP1 and PPARγ, and Figure 11A demonstrates that 5% PEG gels had more UCP-ir and PPARγ-ir cells with greater intensity of staining (brown color), compared to 10% PEG gels. Figure 11B shows levels of adipose-specific and brown adipose-specific gene expression through RT-PCR analysis of RNA from the 3D constructs. The data are represented as fold change in gene expression relative to that of brown ASCs differentiated in 2D culture and harvested at Day 28 of differentiation.

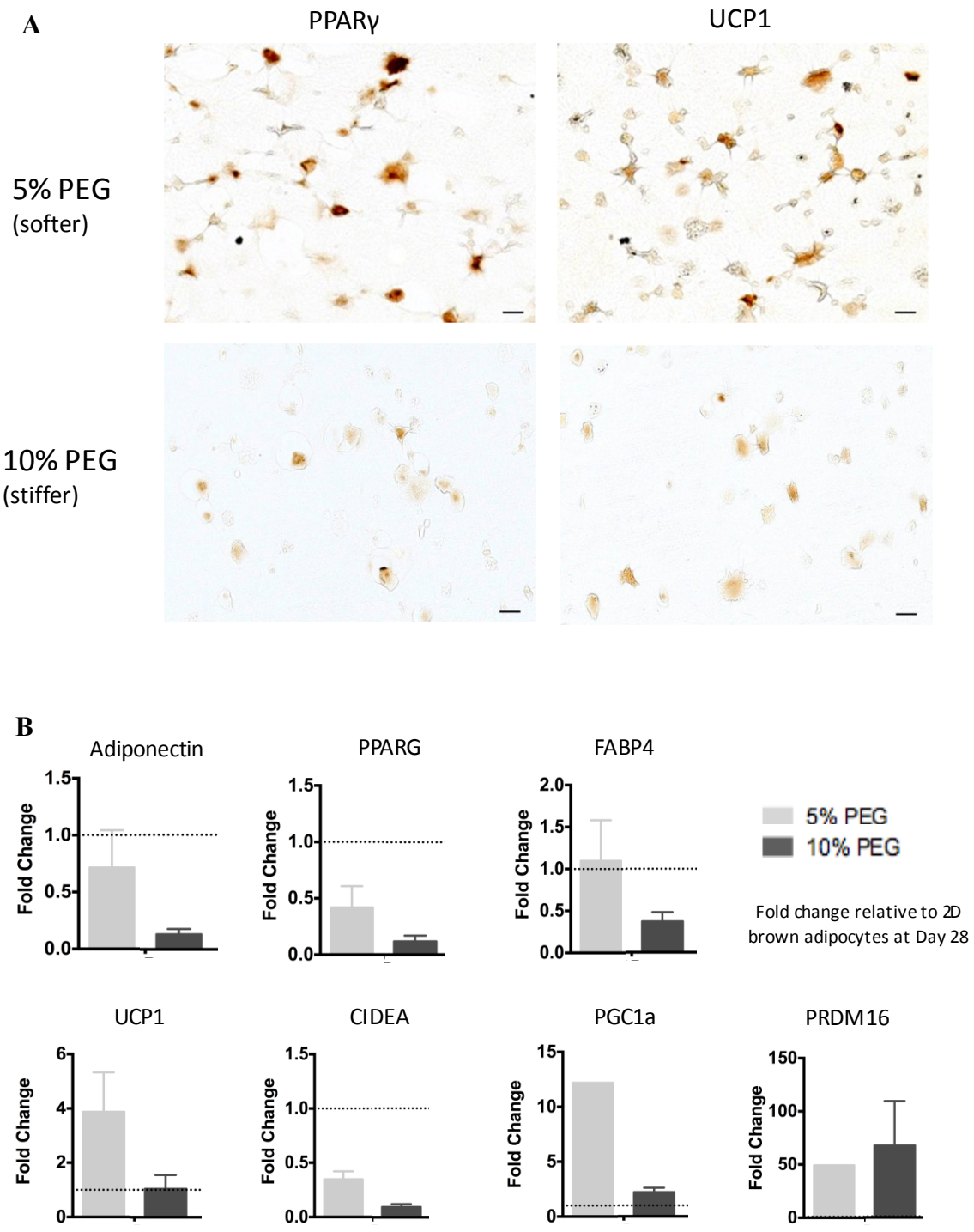

Figure 11: Influence of stiffness of the material on brown adipogenesis of rat brown ASCs. **A**: Immunoreactivity to PPARγ and UCP1 of rat brown ASCs that underwent four weeks of brown adipogenic differentiation in 5% PEG gels or 10% PEG gels. Scale bar = 20 μm. **B**: RT-PCR analysis of RNA from the 3D constructs, represented as fold change in gene expression relative to brown ASCs differentiated in 2D culture and harvested at Day 28 of differentiation.

Regarding the adipose-specific genes adiponectin, PPARγ, and FABP4, cells grown in 3D culture had lower gene expression than those grown in 2D culture (except for FABP4 expression in 5% PEG gels, which was approximately equivalent to 2D culture). However, cells grown in 10% PEG gels had even lower adipose-specific gene expression than those grown in 5% PEG gels. Regarding the brown-adipose specific genes UCP1 and PGC-1α, ASCs differentiated in the softer 5% PEG gels had higher gene expression than those grown in 2D culture. Across the four brown adipose-specific genes, cells grown in 5% PEG gels had higher gene expression than those grown in 10% PEG gels, except for PRDM16, which was higher in 10% PEG gels.

The effect of matrix adhesive properties on brown adipogenesis of rat brown ASCs is described in Figure 12. Rat brown ASCs underwent four weeks of brown adipogenic differentiation in either 5% PEG gels or 10% PEG gels with or without functionalization with the RGD peptide. Figure 12A shows UCP1 and PPARγ immunoreactivity among the constructs, demonstrating that 5% PEG gels without RGD had more UCP-ir and PPARγ-ir cells with greater intensity of staining (brown color), compared to the other gels. Figure 12B compares gene expression among cells grown in the four types of constructs, and the data are represented as fold change in gene expression relative to brown ASCs differentiated in 2D culture and harvested at Day 28 of differentiation. Regarding the adipose-specific genes adiponectin, PPARγ, and FABP4, cells grown in 10% PEG gels, regardless of presence of RGD, had lower adipose-specific gene expression than those grown in 5% PEG gels. Regarding the brown adipose-specific genes UCP1 and PGC-1α, cells grown in 5% PEG gels without RGD had the highest gene expression. Cidea expression was higher in 5% PEG gels than in 10% PEG gels,

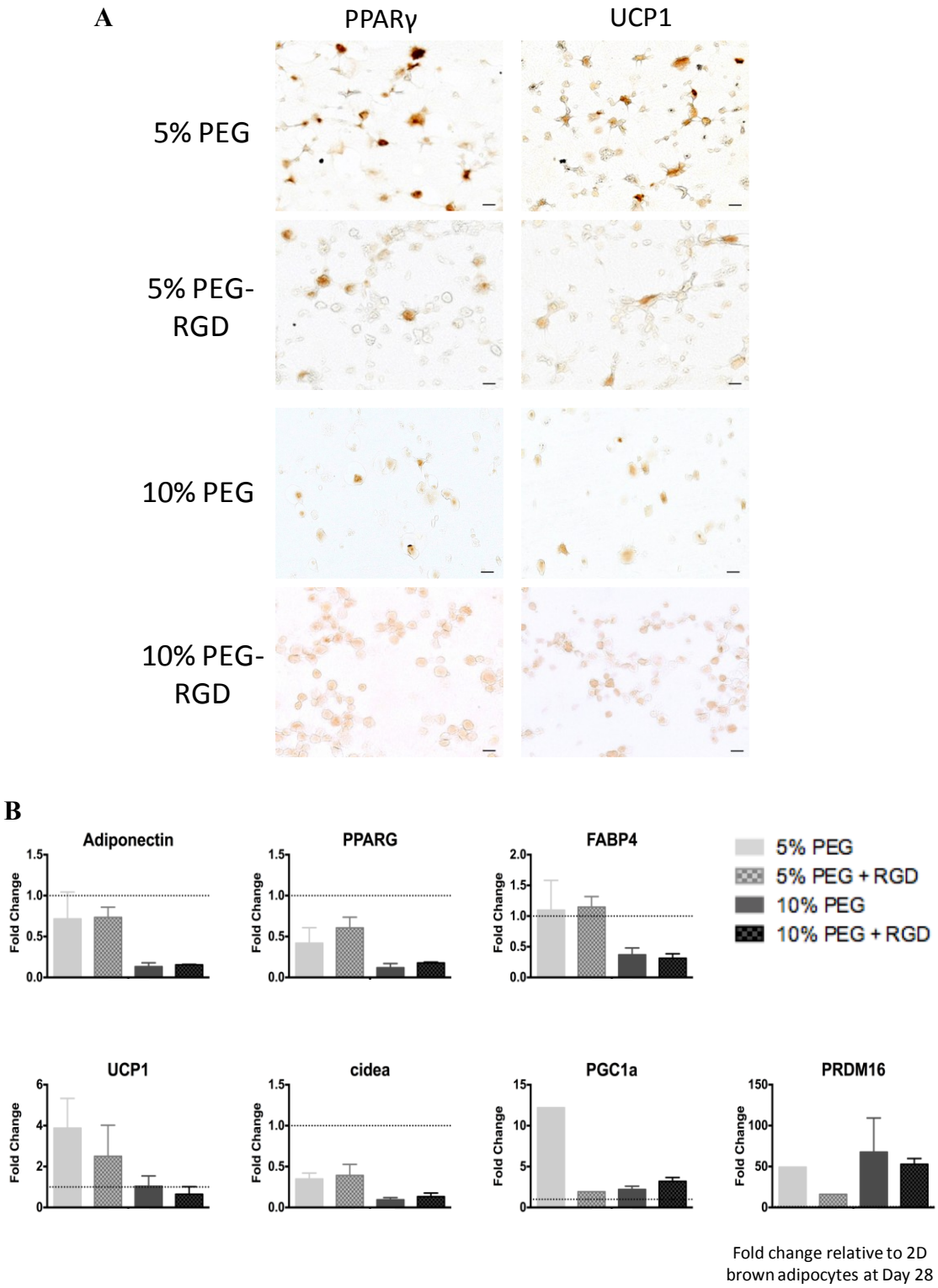

Figure 12: Influence of adhesive properties of the material on brown adipogenesis of rat brown ASCs. **A**: Immunoreactivity to PPARγ and UCP1 of rat brown ASCs that underwent four weeks of brown adipogenic differentiation in 5% PEG gels or 10% PEG gels, with or without RGD. Scale bar = 20 μm. **B**: RT-PCR analysis of RNA from the 3D constructs, represented as fold change in gene expression relative to brown ASCs differentiated in 2D culture and harvested at Day 28 of differentiation.

regardless of presence of the RGD peptide. The 10% PEG gel without RGD had the highest expression of PRDM16, but overall the 5% PEG gel without RGD was most conducive to brown adipogenesis. Across the four brown adipose-specific genes, presence of the RGD peptide either negatively affected gene expression (UCP1, PGC-1α, PRDM16) or did not affect it (Cidea).

The influence of diffusion capability on white and brown adipogenesis was examined initially by constructing either 20 μL or 100 μL volume hydrogels made of 10% PEG. Rat white ASCs and brown ASCs underwent white and brown adipogenesis, and Figure 13A demonstrates the different locations of UCP1-ir and PPARγ-ir cells within the gels, showing variability between the edges and centers of the constructs. In the larger 100 μL constructs containing white ASCs undergoing white or brown adipogenesis, there was a notable difference in PPARγ and UCP1 immunoreactivity (brown color) in cells at the edge of the gel compared to those in the center. This difference was less striking in the brown ASCs undergoing brown adipogenesis and in cells grown in the 20 μL gels. Figure 13B shows gene expression levels between the adipocyte types, examining the effect of hydrogel size. The data are represented as fold change in gene expression relative to the gene expression of the 100 μL constructs containing white ASCs undergoing white adipogenic differentiation. Expression of adiponectin was lower in the smaller constructs that contained white and white-to-brown adipocytes, but otherwise expression of adipose-specific genes (PPARγ and FABP4) was higher in the smaller constructs across all types of adipocytes. UCP1 expression in white-to-brown adipocytes was higher in the smaller constructs, whereas in brown adipocytes it was lower in the

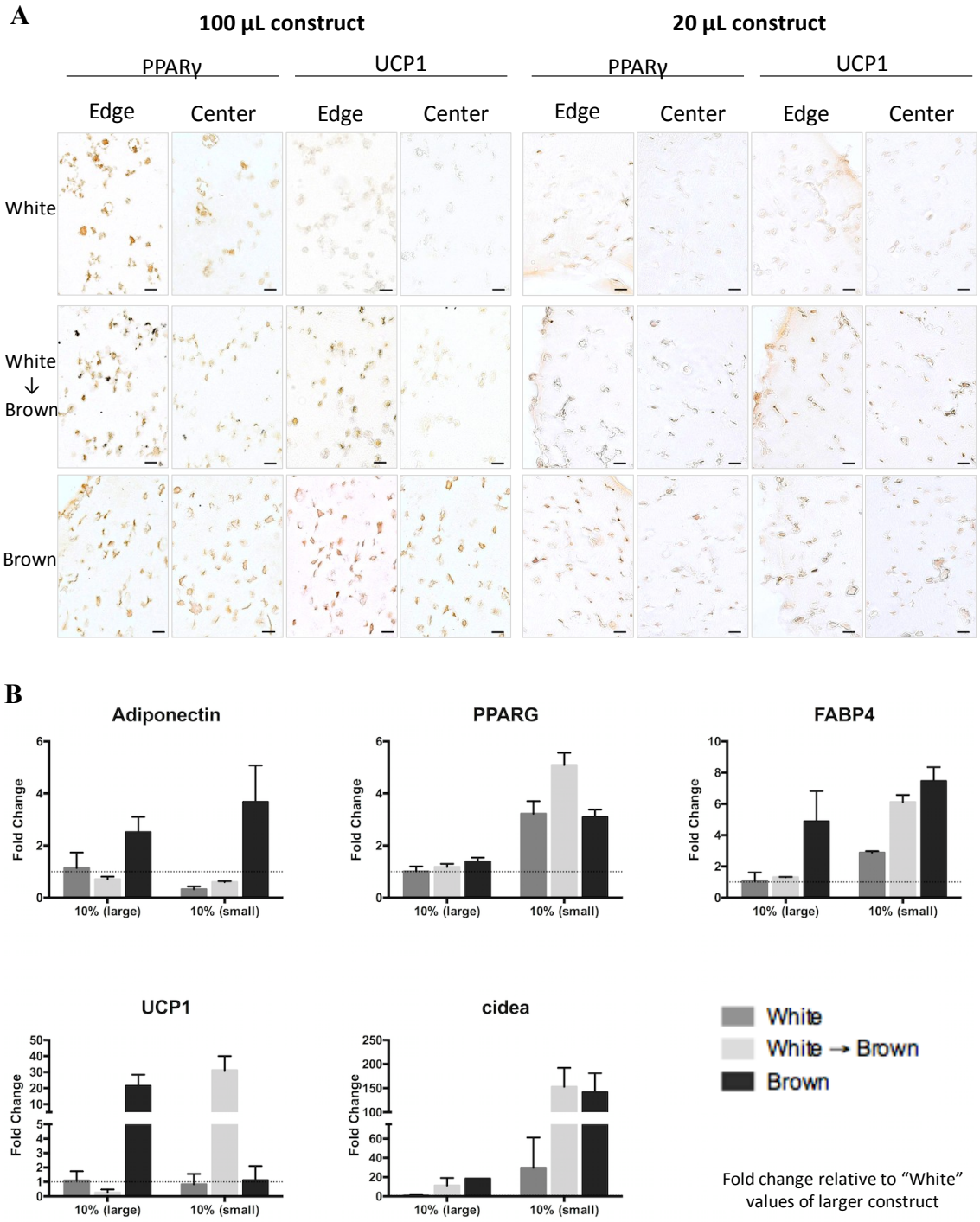

Figure 13: Influence of diffusion capability on adipogenesis in 10% PEG hydrogels, 3 weeks. **A**: Comparison of the location of UCP1-ir and PPARγ-ir cells within gels containing rat white ASCs and brown ASCs that underwent white or brown adipogenic differentiation. The gels were either 100 µL or 20 µL in volume. Scale bar = 20 µm. **B**: RT-PCR analysis of RNA from the 3D constructs is represented as fold change in gene expression relative to the gene expression of the 100 µL constructs containing white ASCs undergoing white adipogenic differentiation. "White" = white adipogenic differentiation of white adipose-derived stem cells. "White → Brown" = brown adipogenic differentiation of white adipose-derived stem cells. "Brown" = brown adipogenic differentiation of brown adipose-derived stem cells.

smaller constructs. Cidea expression was higher in the small constructs across the three types of adipocytes.

As 5% PEG had enhanced brown adipogenesis (Figures 11, 12), the diffusion capability on brown adipogenesis was further examined by differentiating rat brown ASCs to brown adipocytes in 5% PEG gels of either 20 μL or 100 μL in volume. Figure 14A shows immunoreactivity to PPARγ and UCP1 of brown adipocytes, and the images are of sections taken from the center of the gels. The images show that the 20 μL gels had more UCP-ir and PPARγ-ir cells (brown color), compared to the 100 μL gels. Figure 14B compares gene expression between cells in the different sized constructs, represented as fold change in gene expression relative to the larger construct. Regarding the adipose-specific genes adiponectin, PPARγ, and FABP4, cells grown in the smaller constructs had higher gene expression. Regarding the brown adipose-specific genes, the cells grown in the smaller construct had less UCP1 expression and approximately equal cidea expression relative to those grown in the larger construct. Considering the initiative for modifying the material was differentiation down an undesired lineage in the center of the gels, it was determined that the smaller constructs were overall more favorable for brown adipogenesis.

Having determined that 20 μL, 5% PEG gels without RGD functionalization were most conducive to brown adipogenesis of rat brown ASCs, human white ASCs were encapsulated in 20 μL, 5% PEG gels and differentiated to white and brown adipocytes for four weeks. The images in Figure 15A compare the immunoreactivity to PPARγ and UCP1 between human white adipocytes and white-to-brown adipocytes, showing that

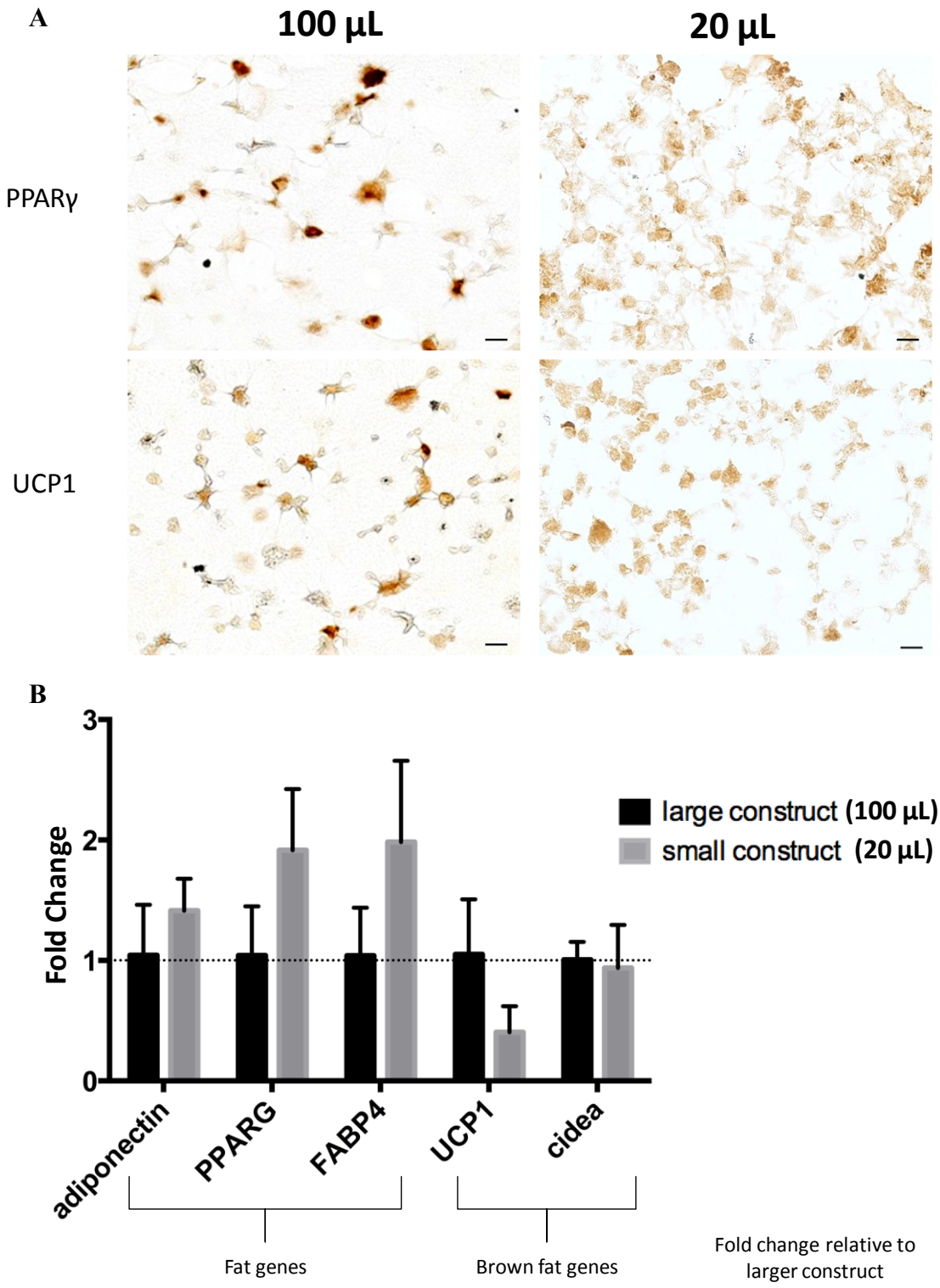

Figure 14: Influence of diffusion capability on brown adipogenesis in 5% PEG hydrogels, 4 weeks. **A**: Comparison of UCP1 and PPARγ immunoreactivity of cells within the center of gels that were either 100 µL or 20 µL in volume. Scale bar = 20 µm. **B**: RT-PCR analysis of RNA from the 3D constructs is represented as fold change in gene expression relative to the larger construct.

gels containing white-to-brown adipocytes had more UCP-ir cells (brown color, right lower image), compared to gels containing white adipocytes. Unlike in 2D, the human white adipocytes were not enriched with UCP1, and the white-to-brown adipocytes had excellent UCP1 immunoreactivity. The difference in UCP1 immunoreactivity between the two types of adipocytes is more striking in this 3D environment than in 2D culture (see Figure 5), and aligns with the expectation that white adipocytes would not express UCP1. Figure 15B describes differences in gene expression, represented as fold change relative to the gene expression of the white adipocytes. The left graph shows changes in adipose-specific genes and the right graph shows changes in brown adipose-specific genes. The white-to-brown adipocytes showed increased expression of the adipose-specific genes adiponectin and FABP4 and of the brown adipose-specific genes UCP1 and cidea (red arrows). The adipocytes had approximately equal expression of adipose-specific PPARγ and brown adipose-specific PGC-1α and PRDM16. Interestingly, these data differ from the relative gene expression in 2D, as the white adipocytes and white-to-brown adipocytes in 2D culture had approximately equivalent expression of UCP1 and cidea after four weeks of differentiation (see Figure 7). The 3D data are more in line with the expectation that the white-to-brown adipocytes would express higher levels of brown adipose-specific genes.

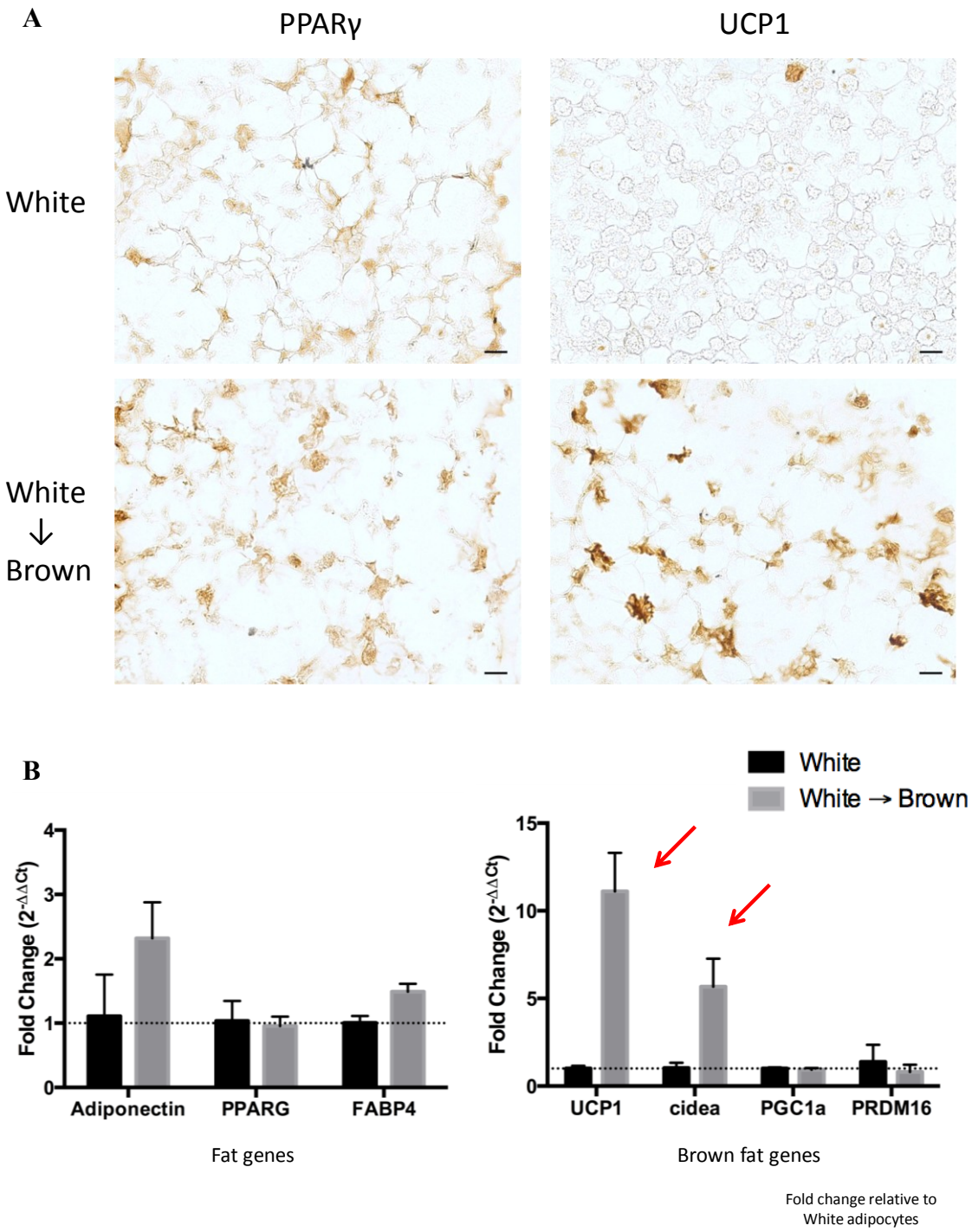

Figure 15: 3D adipogenesis of human ASCs. **A**: Comparison of PPARγ and UCP1 immunoreactivity between human white ASCs that underwent four weeks of either white or brown adipogenesis while encapsulated in 20 µL gels of 5% PEG. Scale bar = 20 µm. **B**: RT-PCR analysis of RNA is represented as fold change relative to the gene expression of the white adipocytes. "White" = white adipogenic differentiation of white adipose-derived stem cells. "White → Brown" = brown adipogenic differentiation of white adipose-derived stem cells.

Evaluation of metabolism in 3D

To characterize the function of adipocytes grown in 3D, the mitochondrial respiratory profiles were assessed. ASCs were encapsulated in 20 μL gels made of 5% PEG and adipogenic differentiation was continued for five weeks before respiration was measured. Figure 16 describes the respiratory profile of rat white ASCs and brown ASCs that underwent white and brown adipogenesis. The basal mitochondrial respiration among the three adipocyte types is shown in Figure 16A. Compared to both white and white-to-brown adipocytes, the brown adipocytes had significantly higher basal mitochondrial respiration. However, no significant difference in basal respiration was exhibited between white and white-to-brown adipocytes. These data differ from the 2D data, where the white-to-brown adipocytes had significantly greater respiration than both the white and the brown adipocytes (see Figure 8). In 3D, the brown adipocytes had significantly higher maximum respiratory capacity than both white and white-to-brown adipocytes (Figure 16B), while the maximum respiratory capacity did not differ significantly between white and white-to-brown adipocytes. Again these data differ from that of the cells grown in monolayer, where the white-to-brown adipocytes had higher maximum respiratory capacity than both white and brown adipocytes (see Figure 8). Although the brown adipocytes had significantly higher maximum respiratory capacity in 3D than white and white-to-brown adipocytes, the differences among the adipocytes' percent spare respiratory capacity were not significant (Figure 16C). These data differ from the 2D data that showed lower percent spare respiratory capacity in white adipocytes compared to both white-to-brown and brown adipocytes (see Figure 8).

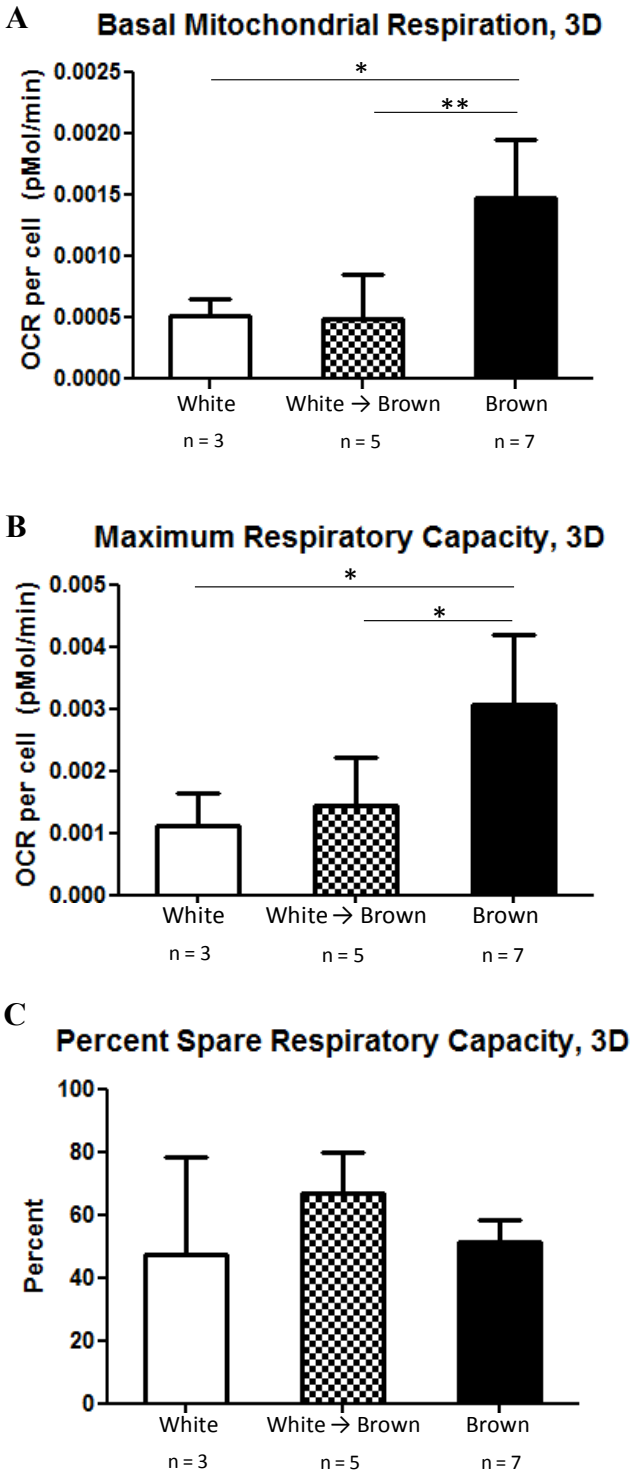

Figure 16: Mitochondrial respiratory profiles of rat adipocytes in 3D. **A**: Comparison of basal mitochondrial respiration among the three types of differentiated adipocytes after 5 weeks of adipogenesis in 20 µL, 5% PEG hydrogels. **B**: Maximum respiratory capacity. **C**: Percent spare respiratory capacity. "White" = white adipogenic differentiation of white ASCs. "White → Brown" = brown adipogenic differentiation of white ASCs. "Brown" = brown adipogenic differentiation of brown ASCs. * : $p < 0.05$; ** : $p < 0.01$.

In Figure 17, the mitochondrial respiratory profile of human white ASCs that underwent white and brown adipogenesis is examined. The basal mitochondrial respiration is described in Figure 17A, which shows that white-to-brown adipocytes had significantly greater basal respiration than the white adipocytes. This is in contrast with the 2D data (see Figure 9), that did not demonstrate a significant difference in basal respiration between white and white-to-brown adipocytes. These 3D data align with our expectation that white-to-brown adipocytes would have higher basal respiration than white adipocytes. Figure 17B evaluates uncoupling, demonstrating that the white-to-brown adipocytes had significantly higher proton leak, meaning they were more uncoupled than the white adipocytes. These data are reversed compared to the 2D data (see Figure 9), but they align with our hypothesis that white-to-brown adipocytes would be more uncoupled than white adipocytes. The white-to-brown adipocytes had significantly higher maximum respiratory capacity than the white adipocytes in 3D (Figure 17C), as opposed to the 2D data that did not show a significant difference between the adipocytes' maximum respiratory capacity (see Figure 9). However, the white adipocytes had significantly higher percent spare respiratory capacity than the white-to-brown adipocytes, which is consistent with the 2D data (see Figure 9). Overall, these data from both rat and human cells indicate that culturing cells in a 3D environment leads to significantly different cell behavior than observed in cells grown in monolayer.

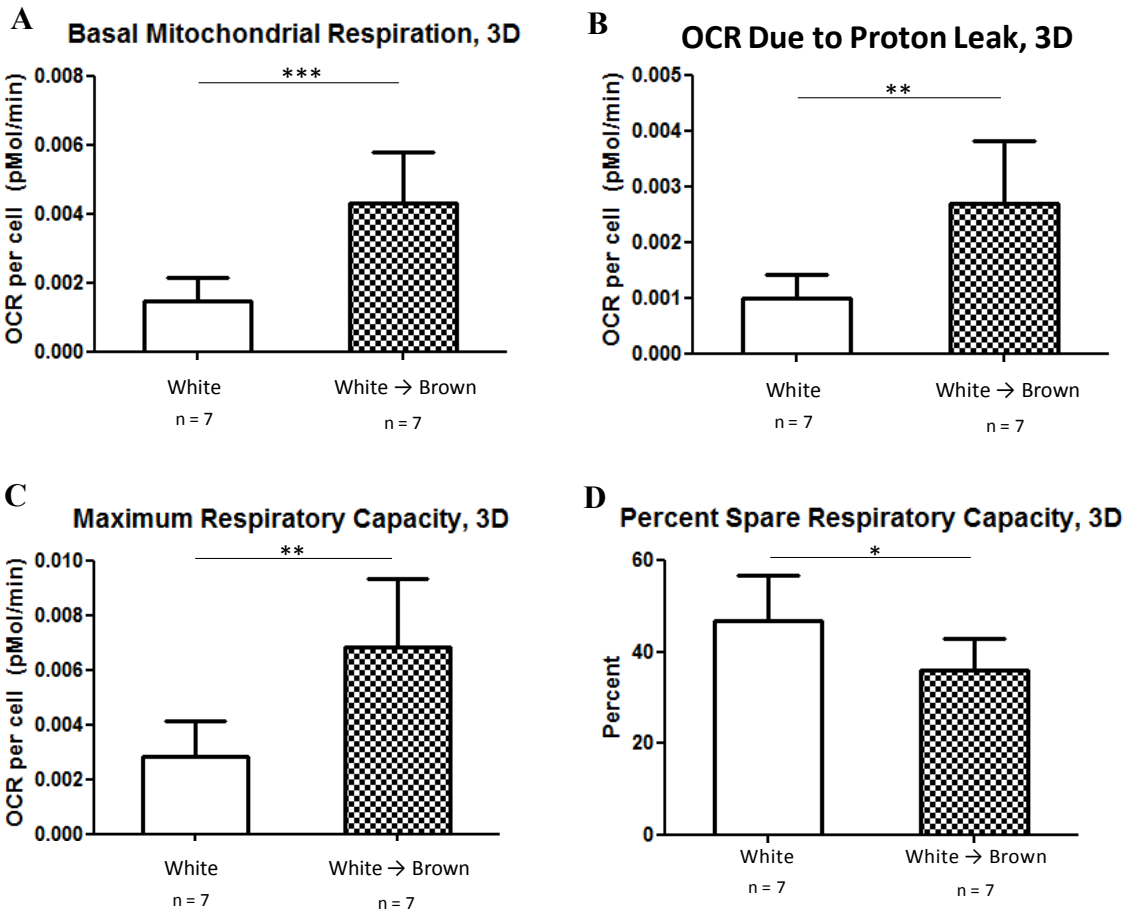

Figure 17: Mitochondrial respiratory profiles of human adipocytes in 3D. **A**: Comparison of basal mitochondrial respiration between the two types of differentiated adipocytes after 5 weeks of adipogenesis in 20 µL, 5% PEG hydrogels. **B**: OCR due to proton leak between white and white-to-brown adipocytes. **C**: Maximum respiratory capacity. **D**: Percent spare respiratory capacity. "White" = white adipogenic differentiation of human white adipose-derived stem cells. "White → Brown" = brown adipogenic differentiation of human white adipose-derived stem cells. * : $p < 0.05$; ** : $p < 0.01$; *** : $p < 0.001$.

DISCUSSION

In the present work, we examined the function of primary rat and human white and brown ASCs, differentiated them to white and brown adipocytes over a month, and measured their mitochondrial respiration. We then differentiated ASCs in 3D synthetic hydrogels and tuned the scaffolds properties to optimize brown adipogenesis. Studying cells in environments that approximate the *in vivo* state is important to be able to extrapolate data for translation to medicine. Tissue engineering uses 3D scaffolds to support and influence cell behavior and allows them to have a more natural morphology than in 2D.

Adipogenesis in monolayer culture

We isolated rat ASCs from brown and white adipose tissue and examined their responses to different concentrations of rat adipose ECM (Figure 1). The basal migration rate of brown and white ASCs was not significantly different, but their responses to ECMs varied. The brown ASCs migrated toward the low concentration of BAT ECM but not the high concentration, which was also true for the white ASCs. Although the composition of BAT ECM was unknown, this phenomenon where the cells did not migrate in response to the high concentration of BAT ECM makes one wonder if the BAT ECM exerts an inhibitory response at a particular concentration. Interestingly, the brown ASCs responded most strongly to the WAT ECM, with the higher WAT ECM concentration eliciting the strongest response of any ECM treatment. Although the white

ASCs also responded to the WAT ECM, the brown ASCs had a significantly stronger response.

ECM contains native proteins and growth factors, and its specific composition is unknown. However, we observed that ECM from BAT and WAT exerted different effects on ASCs, and white and brown ASCs responded differently to the same ECM. White and brown ASCs are derived from different precursor cells (Timmons et al., 2007) and have different functions, so it is reasonable that they would secrete distinct ECMs and have different responses to the same stimulus. Although we only examined migration, future studies could evaluate whether brown or white adipose ECM affect other cell behaviors like growth and differentiation.

We differentiated both rat and human ASCs to white and brown adipocytes using drugs rather than genetic manipulation, and we tracked changes in gene expression over 28 days (Figures 4 and 6), longer than others in the BAT field have done (Hauner et al., 1989; Smih et al., 2002; Tiraby et al., 2003; Seale et al., 2008, 2011; Schulz et al., 2010; Cohen et al., 2014). Rat brown adipocytes had greater expression of adipose-specific and brown-adipose specific genes compared to white adipocytes, and their expression levels continued to increase across four weeks. However, the white adipocytes' expression of adipose-specific genes peaked at day seven or fourteen. The white-to-brown adipocytes expressed adipose-specific and brown adipose-specific genes around the same level as white adipocytes until days 21 and 28 when their expression of brown adipose-specific genes increased. They did not reach the same level as brown adipocytes, but it would be interesting to see how the expression may change with even longer term culture. The human white ASCs that were differentiated to brown adipocytes expressed brown

adipose-specific gene earlier than the white adipocytes, but by day 21 the white adipocytes were expressing BAT-specific genes at the same level (Figure 7). The white adipocytes also showed immunoreactivity to UCP1 (Figure 5).

The changes in levels of brown adipose-specific transcripts that we saw over different time points informs the literature, as others are conducting experiments after a week or less of differentiation, while we have seen changes in gene expression continuing through a month, and it may continue to change beyond four weeks. However, other groups have induced expression of genes through viral delivery systems (Tiraby et al., 2003; Kajimura et al., 2009), so the gene expression and function of those cells may not be comparable to our results. Although the relative gene expression of our rat white-to-brown adipocytes was not striking, they were immunoreactive for UCP1 like the brown adipocytes (Figure 4). Even more interesting was the function of these white-to-brown cells.

We examined cell function through metabolic analysis, measuring their mitochondrial respiration and uncoupling. In the 2D environment, we found that rat brown ASCs had significantly higher mitochondrial respiration than both rat white ASCs and differentiated rat white adipocytes (Figure 8). The rat brown adipocytes had significantly greater basal mitochondrial respiration than white adipocytes, and of particular interest, the white-to-brown adipocytes had significantly greater respiration than both white and brown adipocytes. Further, despite less relative gene expression of UCP1 than brown adipocytes, the white-to-brown adipocytes were more uncoupled than both brown and white adipocytes. This suggests that the relative amount of gene transcripts did not directly translate to function. These white-to-brown cells also had higher maximum respiratory capacity than white or brown adipocytes. Indeed, one cannot always infer

protein expression from mRNA expression, as the relationship between transcription and translation is not linear (Maier et al., 2009). Factors such as translation efficiency, protein stability, and post-translational modification can affect the link between the levels of mRNA and protein expression, and the experimental signal-to-noise ratio can influence the level of transcripts detected.

While the rat white-to-brown adipocytes had significantly different function than the rat white adipocytes, the human white and white-to-brown adipocytes had essentially the same basal mitochondrial respiration (Figure 9). Although they both had increased UCP1 gene expression and showed UCP1-immunoreactivity, the white adipocytes were more uncoupled than the white-to-brown adipocytes. They did not differ in their maximum respiratory capacity, but the white adipocytes had higher percent spare respiratory capacity. This difference between the species is particularly relevant for the field, as much BAT work is done in 2D with mouse or rat cells, and our data shows that the rodent phenotype cannot always be extrapolated to human cell function. Indeed, although rodents and humans share a large percentage of DNA, often data acquired in animal models (rodents and other species) does not predict the human phenotype, with differences in enzyme activity, drug metabolism (Shanks et al., 2009), and oral bioavailability (Musther et al., 2014) becoming especially noticeable when predicting outcomes of clinical trials.

Optimizing the scaffold

As the next step to our innovation, we differentiated these cells in 3D synthetic scaffolds, allowing them to have a more natural spherical shape, rather than be flat on one side and have an artificial polarity imposed by 2D culture. To optimize brown adipogenesis, we tuned scaffold properties, adjusting the stiffness and adhesion of the environment (Figures 11 and 12). Adipogenesis was favored by the softer, 5% PEG gels without the RGD cell adhesion peptide, evidenced by gene expression and immunoreactivity to UCP1. Adipose is a soft tissue, and although our lab has induced white adipogenesis of embryoid body-derived cells and MSCs in 10% PEG gels (Hillel et al., 2009), the best results for brown adipogenesis were seen in the softer 5% gels. In a study in our lab of PEG hydrogels conjugated with CDYRGDS at various concentrations, white adipogenesis was favored on softer hydrogels regardless of the presence of RGD (Singh et al., 2013). While others have seen both enhancement and suppression of adipogenesis from fibronectin (Kubo et al. (2010), in our hands, brown adipogenesis was better in the absence of RGD. A review by Ivaska and Heino (2010) discusses the effect of integrins on cell signaling, asserting that integrin binding can modulate signaling pathways like growth factor receptors do, and some integrins can even bind growth factors. For example, the RGD sequence in transforming growth factor-β (TGF-β) can be bound by αVβ6 integrin. This interaction is relevant for BAT and obesity, as Yadav et al. (2011) demonstrated that inhibiting TGF-β and Smad3 (which regulates TGF-β targets) signaling leads to browning of WAT.

As discussed earlier, tuning scaffold properties to guide cell function is a core practice of tissue engineering. Mechanical feedback from stiff polylactic acid encourages bone and cartilage formation, while the soft Matrigel is preferred for epithelial cells and soft tissue

(Rehfeldt et al., 2007). In recent years, stiffness of the scaffold has been shown to be a significant variable. In a 2008 review, Breuls and colleagues provided discussion of the effect of matrix stiffness on cell function. The elasticity of the environment impacts the cell shape via interactions with the cytoskeleton, and the cell morphology can influence migration, growth, and differentiation. Indeed, the stiffness of the scaffold can serve as a variable to steer cell behavior and can reduce the need for bioactive compounds.

Engler et al. (2006) cultured bone marrow-derived mesenchymal stem cells (MSC) on polyacrylamide scaffolds with different amounts of acrylamide crosslinking to generate constructs with different elasticities. They examined cell morphology and gene transcription, finding that the lineage toward which MSCs differentiated was strongly influenced by the stiffness of the scaffold, with softer scaffolds encouraging neurogenesis and stiffer scaffolds leading to osteogenesis. The authors found that the longer the cells were grown on a particular scaffold, the more committed they were toward a lineage, evidence by diminished responses to differentiation media toward a different lineage. For example, MSCs grown on a soft scaffold with only growth medium express β3 tubulin, a marker of neurogenesis. While their β3 tubulin levels will decrease when given osteogenic or myogenic medium after one week of culture on a soft scaffold, the β3 tubulin levels do not change when given such induction medium after three weeks of growth on a soft scaffold. Those results suggest that with enough time, the elasticity of the scaffold can exert a more powerful influence on differentiation than induction agents. Our work shows less dramatic evidence of the effect of scaffold stiffness on differentiation, but it lends evidence to the idea that optimization of the matrix is necessary for steering appropriate differentiation.

Challenges with nutrient diffusion

We also altered the size of the constructs to explore the effect of diffusion capacity (Figures 13 and 14). Brown adipogenesis was enhanced in the smaller constructs, suggesting that improved diffusion and access to oxygen and nutrients was important for differentiation to brown adipocytes. This was striking in the *in vivo* study (Figure 10), where despite four weeks of *in vitro* adipogenesis, cells in the center of the hydrogels underwent osteogenesis after implantation in the animals. The constructs were not vascularized, so unlike the *in vitro* culture conditions, they had limited access to nutrients and oxygen. Indeed, others have shown that bone marrow-derived MSCs have improved osteogenesis and impaired adipogenesis in low oxygen environments (Hung et al., 2012). Our results show that the microenvironment can steer differentiation more strongly than four weeks of exposure to adipogenic drugs. We know that BAT is highly metabolically active, and our results suggest that it may be difficult to scale up the size of our synthetic tissues unless the diffusion limitations are overcome. Indeed, delivery of nutrients and elimination of waste products in artificial tissues is a hurdle for tissue engineering in general.

When cells are cultured in 3D, the peripheral cells have better access to nutrients and ability to remove waste. However, the limiting factor with 3D *in vitro* culture is usually access to oxygen (Martin and Vermette, 2005; Mazzoleni et al., 2009). Cells in the center of a construct can be at risk of undergoing apoptosis due to hypoxia, and as cells deposit ECM, diffusion is reduced (Bland et al., 2013). Beyond inducing apoptosis of

central cells, hypoxia also induces changes in cell metabolism and function (Bland et al., 2013), so impaired oxygenation of part of a construct can skew results of an experiment. Another consideration is the different oxygen tension that cells would experience *in vivo* compared to *in vitro*. While *in vitro* conditions expose cells to atmospheric oxygen (160 mmHg), physiological oxygen tension is closer to 40 mmHg in most tissues and transplanted cells may not survive such a drastic change in oxygenation (Bland et al., 2013).

A perfused bioreactor is a system of growing cells in 3D, where a vessel containing cells rotates and medium continually flows through the system (Frye and Patrick, 2006). Perfusion bioreactors can improve nutrient delivery and oxygenation throughout a construct. Frye and Patrick (2006) cultured preadipocytes in perfused bioreactors and found that cells were able to differentiate and form tissue-like clusters. Importantly, these aggregates had living adipocytes throughout, with no central necrosis, and the authors created tissues as large as 4-5 mm in diameter in three weeks. However, two weeks after implantation in rats the artificial tissue had been adsorbed. If this technique could be scaled up, it may be useful for creating a large enough piece of artificial adipose to fill a tissue defect, although the tissue would need to persist *in vivo* longer. Further, it is unclear whether a large piece of tissue could survive outside of the bioreactor without immediate vascular access *in vivo*.

Stosich et al. (2007) created PEG hydrogels with microchannels through them and implanted them in immunocompromised mice. Some hydrogels also contained bFGF, with and without microchannels. After 4 weeks, host tissue had infiltrated the microchannels, but in the bFGF-only gels, host tissue had penetrated the construct,

despite lack of channels, and the tissue resembled blood vessels. The authors also encapsulated human bone marrow-derived MSCs in these gels with or without 1 week of adipogenic differentiation, and then implanted them in mice. Only gels that contained pre-differentiated cells produced adipocytes *in vivo*, but their work showed that providing conduits and bioactive molecules in the scaffold can promote host cell infiltration, which is an important step in regenerative medicine.

Altered metabolism in 3D environment

When we had determined which scaffold enhanced brown adipogenesis, measured by increases in gene transcripts and immunoreactivity to UCP1, we analyzed mitochondrial respiration. Strikingly, the metabolic profiles differed in 3D compared to 2D for both rat and human cells.

In 3D, although the rat white-to-brown adipocytes had increased expression of BAT-specific genes (seem in the small construct of 10% PEG, as only brown ASCs were tested in 5% PEG), they had dramatically different function compared to 2D, as they essentially acted like white adipocytes (Figure 16). Their basal respiration, maximal respiration, and percent spare respiratory capacity did not differ from the white adipocytes, while the brown adipocytes had higher basal respiration and maximal respiration. However, the human white-to-brown adipocytes had higher expression of the BAT-specific genes UCP1 and cidea in 3D, and they were immunoreactive to UCP1 while the white adipocytes were not (Figure 15). These data are in contrast to the 2D data that showed white adipocytes expressing BAT genes. The contrasts between 2D and 3D continued

when analyzing the cell function (Figure 17), as the human white-to-brown adipocytes now had significantly higher basal respiration than the white adipocytes, were significantly more uncoupled, and had greater maximum respiratory capacity. The white adipocytes had higher percent spare respiratory capacity.

Together these data show that cell function changes based on the environment, with both rat and human cells having different metabolic profiles and gene expression in 2D versus 3D environments. Further, the rat and human cells differed from each other in their function, regardless of the environment, which makes extrapolating rat data to the human condition challenging. The goal of research is to gain insight into human normal biology and disease states, and our work demonstrates that in the case of brown adipose research, using rat cells may not inform human biology. Since translating research to medicine also means treating 3D tissues, it follows that lab research should ideally be conducted in 3D models in addition to *in vivo* work. If the data in 2D and 3D vary in other cell types as significantly as it did in our work, then it seems imperative that cells be studied in 3D before being tested *in vivo*.

Our constructs were optimized for brown adipogenesis of rat brown ASCs. Perhaps to encourage brown adipogenesis of rat white ASCs, the scaffold properties need to be altered. However, our interest is in translational research, and the human ASCs underwent brown adipogenesis and functioned significantly differently than white adipocytes. They had higher basal respiration and were uncoupled, which means they were acting more like brown adipocytes. If one wanted to implant engineered brown adipose into a human, then having human ASCs functioning like brown adipose within a synthetic scaffold is a step in the right direction. Although not immediately translatable,

our technique could be used to create synthetic human BAT for drug testing. To our knowledge, this is the first creation of 3D BAT, and we have engineered it using ASCs from primary tissue without conducting genetic manipulation of the cells. This further informs the literature, as the work in the BAT field is done in 2D, yet our results demonstrate a different functional phenotype when cells are grown in 3D, which is closer to their natural environment. Cell morphology can alter cell function as we have seen, and as discussed, this phenomenon is supported by work from others in tissue engineering.

Future translation

Animal models are used before human trials of therapeutic interventions, but often animals are used based on experimentation on cells grown in monolayer. As discussed earlier and as seen in our work, cell behavior can be altered when cultured in 3D compared to 2D. As a bridge from 2D to animal work, 3D studies could be used, and their better resemblance to the *in vivo* environment may improve the likelihood of a favorable outcome when translating work to animal studies. Further, 3D models can be constructed from human cells, eliminating inter-species differences. Beyond use as a pre-animal study tool, 3D work can also be used for drug testing (Mazzoleni et al., 2009).

In obesity, energy intake is greater than energy expenditure, and BAT has the potential to serve as energy sink and improve glucose tolerance. If one can harvest ASCs, differentiate them into brown adipocytes, and return them to the body, they may be able to burn excess calories and serve as a weight-loss tool. For human translation,

differentiation of white ASCs to brown adipocytes is a more feasible approach than trying to acquire brown ASCs due to the abundance and relative ease of acquisition of white adipose tissue. In our hands, ASCs from human subcutaneous fat are capable of differentiating into brown adipocytes without use of viral vectors. In a review by Gimble et al. (2011), the authors discuss use of ASCs in clinical trials and the stringent criteria that must be met to meet current Good Manufacturing Practices (cGMP). Most academic facilities do not meet cGMP due to practical and financial considerations, but it is wise to be aware of the criteria to minimize alterations to protocols when translating research to human subjects. Clinical use of ASCs has largely been in breast reconstruction and GI-GU fistula repair, performing autologous transfer of ASCs, and clinical trials have been limited to examining safety of ASCs. Indeed, cell-based therapy is still transitioning from preclinical to clinical application.

Although β3-adrenergic agonists have reduced the impact of high fat diet on adiposity in rodents (Ghorbani et al., 1997), their usefulness for treating obesity in humans is likely limited. In a review by Ursino et al. (2009), other organs that express the β3-adrenergic receptor are highlighted, such as the brain, bladder, heart, and GI tract. Although having other targets may broaden the usefulness of these agonists for treating other disease, reduced specificity increases the likelihood for side effects. Further, clinical trials of β3-adrenergic receptor agonists did not show the same desirable metabolic effects in humans that were observed in rodents.

As discussed earlier, while studying transgenic mice (Seale et al., 2008, 2011) or using viral vectors to deliver genes of interest (Tiraby et al., 2003; Kajimura et al., 2009) can present advantages for studying BAT regulation, the ability to translate such work to

clinical use may be limited. Rather than using a global approach to stimulate existing BAT, which may have adverse effects on other organ systems, we propose that a better way to leverage BAT to address excess caloric imbalance is to increase the amount of BAT using tissue engineering techniques, which have not previously been applied to the BAT field. As clinical use of ASCs is still in its infancy, an alternative to cell-based therapy could be induction of UCP1 expression in native WAT, such as through a local, drug-eluting implant. However, the efficacy may be low if one must rely on differentiation of nearby ASCs, although there is some evidence that mature white adipocytes can transdifferentiate (Frontini and Cinti, 2010).

By leveraging the tissue engineering technique of growing cells on scaffolds made of synthetic polymers, scientists have been attempting to create artificial tissues for many years (Rehfeldt et al., 2007). To translate discoveries to human applications, researchers must integrate basic cell biology research and tissue engineering with knowledge of clinical needs and requirements. It is important to understand the limitations and capabilities of each field while we work together to transform regenerative medicine.

REFERENCES

Agilent Technologies (2016) Website: "How Seahorse XF Analyzers Work." http://www.agilent.com/en-us/products/cell-analysis-(seahorse)/how-seahorse-xf-analyzers-work. Accessed 6/17/16.

Austin S and St-Pierre J. (2012) PCG1α and mitochondrial metabolism - emerging concepts and relevance in ageing and neurodegenerative disorders. *J Cell Sci*. Nov 1;125(Pt 21):4963-71.

Baumruk F, Flachs P, Horáková M, Floryk D, Kopecký J. (1999) Transgenic UCP1 in white adipocytes modulates mitochondrial membrane potential. *FEBS Lett*. Feb 12;444(2-3):206-10.

Bland E, Dréau D, Burg KJ. (2013) Overcoming hypoxia to improve tissue-engineering approaches to regenerative medicine. *J Tissue Eng Regen Med*. Jul;7(7):505-14.

Breuls RG, Jiya TU, Smit TH. (2008) Scaffold stiffness influences cell behavior: opportunities for skeletal tissue engineering. *Open Orthop J*. May 29;2:103-9.

Cannon B and Nedergaard J. (2004) Brown adipose tissue: Function and physiological significance. *Physiol Rev*. 84:277-359.

Carvalho SD, Bianco AC, Silva JE. (1996) Effects of hypothyroidism on brown adipose tissue adenylyl cyclase activity. *Endocrinology*. Dec;137(12):5519-29.

Cederberg A, Grønning LM, Ahrén B, Taskén K, Carlsson P, Enerbäck S. (2001) FOXC2 is a winged helix gene that counteracts obesity, hypertriglyceridemia, and diet-induced insulin resistance. *Cell*. Sep 7;106(5):563-73.

Cinti S. (2006) Functional Anatomy of the "Adipose Organ". In G. Mantovani (Ed.), *Cachexia and Wasting: A Modern Approach* (pp 3-22). Milan, Italy: Springer-Verlag Italia.

Cohen P, Levy JD, Zhang Y, Frontini A, Kolodin DP, Svensson KJ, Lo JC, Zeng X, Ye L, Khandekar MJ, Wu J, Gunawardana SC, Banks AS, Camporez JP, Jurczak MJ, Kajimura S, Piston DW, Mathis D, Cinti S, Shulman GI, Seale P, Spiegelman BM. (2014) Ablation of PRDM16 and beige adipose causes metabolic dysfunction and a subcutaneous to visceral fat switch. *Cell*. Jan 16;156(1-2):304-16.

Crane JD, Palanivel R, Mottillo EP, Bujak AL, Wang H, Ford RJ, Collins A, Blümer RM, Fullerton MD, Yabut JM, Kim JJ, Ghia JE, Hamza SM, Morrison KM, Schertzer JD, Dyck JR, Khan WI, Steinberg GR. (2015) Inhibiting peripheral serotonin synthesis reduces obesity and metabolic dysfunction by promoting brown adipose tissue thermogenesis. *Nat Med*. Feb;21(2):166-72.

Cypess AM, Lehman S, Williams G, Tal I, Rodman D, Goldfine AB, Kuo FC, Palmer EL, Tseng YH, Doria A, Kolodny GM, Kahn CR. (2009) Identification and importance of brown adipose tissue in adult humans. *N Engl J Med*. 360:1509–1517.

Divakaruni AS, Rogers GW, Murphy AN. (2014) Measuring Mitochondrial Function in Permeabilized Cells Using the Seahorse XF Analyzer or a Clark-Type Oxygen Electrode. *Curr Protoc Toxicol*. May 27;60:25.2.1-16.

Driskell RR, Lichtenberger BM, Hoste E, Kretzschmar K, Simons BD, Charalambous M, Ferron SR, Herault Y, Pavlovic G, Ferguson-Smith AC, Watt FM. (2013) Distinct fibroblast lineages determine dermal architecture in skin development and repair. *Nature*. Dec 12;504(7479):277-81.

Engler AJ, Sen S, Sweeney HL, Discher DE. (2006) Matrix elasticity directs stem cell lineage specification. *Cell*. Aug 25;126(4):677-89.

Farnier C, Krief S, Blache M, Diot-Dupuy F, Mory G, Ferre P, Bazin R. (2003) Adipocyte functions are modulated by cell size change: potential involvement of an integrin/ERK signalling pathway. *Int J Obes Relat Metab Disord*. Oct;27(10):1178-86.

Freestone PS, Chung KK, Guatteo E, Mercuri NB, Nicholson LF, Lipski J. (2009) Acute action of rotenone on nigral dopaminergic neurons--involvement of reactive oxygen species and disruption of Ca2+ homeostasis. *Eur J Neurosci*. Nov;30(10):1849-59.

Frontini A and Cinti S. (2010) Distribution and development of brown adipocytes in the murine and human adipose organ. *Cell Metab*. Apr 7;11(4):253-6.

Frye CA and Patrick CW. (2006) Three-dimensional adipose tissue model using low shear bioreactors. *In Vitro Cell Dev Biol Anim*. May-Jun;42(5-6):109-14.

Ghorbani M, Claus TH, Himms-Hagen J. (1997) Hypertrophy of brown adipocytes in brown and white adipose tissues and reversal of diet-induced obesity in rats treated with a beta3-adrenoceptor agonist. *Biochem Pharmacol*. Jul 1;54(1):121-31.

Gimble JM, Bunnell BA, Chiu ES, Guilak F. (2011) Concise review: Adipose-derived stromal vascular fraction cells and stem cells: let's not get lost in translation. *Stem Cells*. May;29(5):749-54.

Gimble JM, Katz AJ, Bunnell BA. (2007) Adipose-Derived Stem Cells for Regenerative Medicine. *Circ Res.* 100:1249-1260.

Gnad T, Scheibler S, von Kügelgen I, Scheele C, Kilić A, Glöde A, Hoffmann LS, Reverte-Salisa L, Horn P, Mutlu S, El-Tayeb A, Kranz M, Deuther-Conrad W, Brust P, Lidell ME, Betz MJ, Enerbäck S, Schrader J, Yegutkin GG, Müller CE, Pfeifer A. (2014)

Adenosine activates brown adipose tissue and recruits beige adipocytes via A2A receptors. *Nature*. Dec 18;516(7531):395-9.

Hauner H, Entenmann G, Wabitsch M, Gaillard D, Ailhaud G, Negrel R, Pfeiffer EF. (1989) Promoting effect of glucocorticoids on the differentiation of human adipocyte precursor cells cultured in a chemically defined medium. *J Clin Invest*. Nov;84(5):1663-70.

Hench LL and Polak JM. (2002) Third-generation biomedical materials. *Science*. Feb 8;295(5557):1014-7.

Hillel AT, Varghese S, Petsche J, Shamblott MJ, Elisseeff JH. (2009) Embryonic germ cells are capable of adipogenic differentiation in vitro and in vivo. *Tissue Eng Part A*. Mar;15(3):479-86.

Hillel AT and Elisseeff JH. (2010) Embryonic Progenitor Cells in Adipose Tissue Engineering. *Facial Plast Surg*. Oct;26(5):405-12.

Hoffman AS. (2001) Hydrogels for biomedical applications. *Ann N Y Acad Sci*. Nov;944:62-73.

Hotamisligil GS, Johnson RS, Distel RJ, Ellis R, Papaioannou VE, Spiegelman BM. (1996) Uncoupling of obesity from insulin resistance through a targeted mutation in aP2, the adipocyte fatty acid binding protein. *Science*. Nov 22;274(5291):1377-9.

Hui X, Gu P, Zhang J, Nie T, Pan Y, Wu D, Feng T, Zhong C, Wang Y, Lam KS, Xu A. (2015) Adiponectin Enhances Cold-Induced Browning of Subcutaneous Adipose Tissue via Promoting M2 Macrophage Proliferation. *Cell Metab*. Aug 4;22(2):279-90.

Hung SP, Ho JH, Shih YR, Lo T, Lee OK. (2012) Hypoxia promotes proliferation and osteogenic differentiation potentials of human mesenchymal stem cells. *J Orthop Res*. Feb;30(2):260-6.

Ivaska J and Heino J. (2010) Interplay between cell adhesion and growth factor receptors: from the plasma membrane to the endosomes. *Cell Tissue Res*. Jan;339(1):111-20.

Jastroch M, Divakaruni AS, Mookerjee S, Treberg JR, Brand MD. (2010) Mitochondrial proton and electron leaks. *Essays Biochem*. 47:53-67.

Jones JR, Barrick C, Kim KA, Lindner J, Blondeau B, Fujimoto Y, Shiota M, Kesterson RA, Kahn BB, Magnuson MA. (2005) Deletion of PPARgamma in adipose tissues of mice protects against high fat diet-induced obesity and insulin resistance. *Proc Natl Acad Sci U S A*. Apr 26;102(17):6207-12.

Kajimura S, Seale P, Kubota K, Lunsford E, Frangioni JV, Gygi SP, Spiegelman BM. (2009) Initiation of myoblast to brown fat switch by a PRDM16-C/EBP-beta transcriptional complex. *Nature*. Aug 27;460(7259):1154-8.

Kajimura S, Seale P, Spiegelman BM. (2010) Transcriptional control of brown fat development. *Cell Metab*. Apr 7;11(4):257-62.

Kang X, Xie Y, Powell HM, James Lee L, Belury MA, Lannutti JJ, Kniss DA. (2007) Adipogenesis of murine embryonic stem cells in a three-dimensional culture system using electrospun polymer scaffolds. *Biomaterials*. Jan;28(3):450-8.

Kimura Y, Ozeki M, Inamoto T, Tabata Y. (2002) Time course of de novo adipogenesis in matrigel by gelatin microspheres incorporating basic fibroblast growth factor. *Tissue Eng*. Aug;8(4):603-13.

Kopecky J, Rossmeisl M, Hodný Z, Syrový I, Horáková M, Kolárová P. (1996) Reduction of dietary obesity in aP2-Ucp transgenic mice: mechanism and adipose tissue morphology. *Am J Physiol*. May;270(5 Pt 1):E776-86.

Kubo Y, Kaidzu S, Nakajima I, Takenouchi K, Nakamura F. (2000) Organization of extracellular matrix components during differentiation of adipocytes in long-term culture. *In Vitro Cell Dev Biol Anim*. Jan;36(1):38-44.

Lee JY, Takahashi N, Yasubuchi M, Kim YI, Hashizaki H, Kim MJ, Sakamoto T, Goto T, Kawada T. (2012) Triiodothyronine induces UCP-1 expression and mitochondrial biogenesis in human adipocytes. *Am J Physiol Cell Physiol*. Jan 15;302(2):C463-72.

Lee P, Swarbrick MM, Zhao JT, Ho KKY. (2011) Inducible brown adipogenesis of supraclavicular fat in adult humans. *Endocrinology*, 152(10):3597–3602.

Leonardsson G, Steel JH, Christian M, Pocock V, Milligan S, Bell J, So PW, Medina-Gomez G, Vidal-Puig A, White R, Parker MG. (2004) Nuclear receptor corepressor RIP140 regulates fat accumulation. *Proc Natl Acad Sci* U S A. 2004 Jun 1;101(22):8437-42.

Lidell ME, Betz MJ, Dahlqvist Leinhard O, Heglind M, Elander L, Slawik M, Mussack T, Nilsson D, Romu T, Nuutila P, Virtanen KA, Beuschlein F, Persson A, Borga M, Enerbäck S. (2013) Evidence for two types of brown adipose tissue in humans. *Nat Med*. May;19(5):631-4.

Lin J, Wu PH, Tarr PT, Lindenberg KS, St-Pierre J, Zhang CY, Mootha VK, Jäger S, Vianna CR, Reznick RM, Cui L, Manieri M, Donovan MX, Wu Z, Cooper MP, Fan MC, Rohas LM, Zavacki AM, Cinti S, Shulman GI, Lowell BB, Krainc D, Spiegelman BM.

(2004) Defects in adaptive energy metabolism with CNS-linked hyperactivity in PGC-1alpha null mice. *Cell*. Oct 1;119(1):121-35.

Liu J, DeYoung SM, Zhang M, Zhang M, Cheng A, Saltiel AR. (2005) Changes in integrin expression during adipocyte differentiation. *Cell Metab*. Sep;2(3):165-77.

Lowell BB, S-Susulic V, Hamann A, Lawitts JA, Himms-Hagen J, Boyer BB, Kozak LP, Flier JS. (1993) Development of obesity in transgenic mice after genetic ablation of brown adipose tissue. *Nature*. Dec 23-30;366(6457):740-2.

Ma X, Jin M, Cai Y, Xia H, Long K, Liu J, Yu Q, Yuan J. (2011) Mitochondrial electron transport chain complex III is required for Antimycin A to inhibit autophagy. *Chem Biol*. Nov 23;18(11):1474-81.

Maier T, Güell M, Serrano L. (2009) Correlation of mRNA and protein in complex biological samples. *FEBS Lett*. Dec 17;583(24):3966-73.

Mariman EC and Wang P. (2010) Adipocyte extracellular matrix composition, dynamics and role in obesity. *Cell Mol Life Sci*. Apr;67(8):1277-92.

Martin Y and Vermette P. (2005) Bioreactors for tissue mass culture: design, characterization, and recent advances. *Biomaterials*. Dec;26(35):7481-503.

Mazzoleni G, Di Lorenzo D, Steimberg N. (2009) Modelling tissues in 3D: the next future of pharmaco-toxicology and food research? *Genes Nutr*. Mar;4(1):13-22.

Mizuno H, Tobita M, Uysal AC. (2012) Concise review - adipose-derived stem cells as a novel tool for future regenerative medicine. *Stem Cells*. May;30(5):804-10.

Musther H, Olivares-Morales A, Hatley OJ, Liu B, Rostami Hodjegan A. (2014) Animal versus human oral drug bioavailability: do they correlate? *Eur J Pharm Sci*. Jun 16;57:280-91.

Nicolas A and Safran SA. (2006) Limitation of cell adhesion by the elasticity of the extracellular matrix. *Biophys J*. Jul 1;91(1):61-73.

Ohno H, Shinoda K, Spiegelman BM, Kajimura S. (2012) PPARγ agonists induce a white-to-brown fat conversion through stabilization of PRDM16 protein. *Cell Metab*. Mar 7;15(3):395-404.

Ohno H, Shinoda K, Ohyama K, Sharp LZ, Kajimura S. (2013) EHMT1 controls brown adipose cell fate and thermogenesis through the PRDM16 complex. *Nature*. Dec 5;504(7478):163-7.

Ouellet V, Labbé SM, Blondin DP, Phoenix S, Guérin B, Haman F, Turcotte EE, Richard D, Carpentier AC. (2012) Brown adipose tissue oxidative metabolism contributes to energy expenditure during acute cold exposure in humans. *J Clin Invest*. Feb;122(2):545-52.

Patel PN, Gobin AS, West JL, Patrick CW Jr. (2005) Poly(ethylene glycol) hydrogel system supports preadipocyte viability, adhesion, and proliferation. *Tissue Eng*. Sep-Oct;11(9-10):1498-505.

Prunet-Marcassus B, Cousin B, Caton D, André M, Pénicaud L, Casteilla L. (2006) From heterogeneity to plasticity in adipose tissues: site-specific differences. *Exp Cell Res*. Apr 1;312(6):727-36.

Rehfeldt F, Engler AJ, Eckhardt A, Ahmed F, Discher DE. (2007) Cell responses to the mechanochemical microenvironment--implications for regenerative medicine and drug delivery. *Adv Drug Deliv Rev*. Nov 10;59(13):1329-39.

Reid B, Afzal JM, McCartney AM, Abraham MR, O'Rourke B, Elisseeff JH. (2013) Enhanced tissue production through redox control in stem cell-laden hydrogels. *Tissue Eng Part A*. Sep;19(17-18):2014-23.

Richard D. and Picard F. (2011) Brown fat biology and thermogenesis. *Front Biosci (Landmark Ed)*. Jan 1;16:1233-60.

Rossmeisl M, Barbatelli G, Flachs P, Brauner P, Zingaretti MC, Marelli M, Janovská P, Horáková M, Syrový I, Cinti S, Kopecký J. (2002) Expression of the uncoupling protein 1 from the aP2 gene promoter stimulates mitochondrial biogenesis in unilocular adipocytes in vivo. *Eur J Biochem*. Jan;269(1):19-28.

Saito M, Okamatsu-Ogura Y, Matsushita M, Watanabe K, Yoneshiro T, Nio-Kobayashi J, Iwanaga T, Miyagawa M, Kameya T, Nakada K, Kawai Y, Tsujisaki M. (2009) High incidence of metabolically active brown adipose tissue in healthy adult humans: effects of cold exposure and adiposity. *Diabetes*. 2009 Jul;58(7):1526-31.

Schulz TJ, Huang TL, Tran TT, Zhang H, Townsend KL, Shadrach JL, Cerletti M, McDougall LE, Giorgadze N, Tchkonia T, Schrier D, Falb D, Kirkland JL, Wagers AJ, Tseng YH. (2011) Identification of inducible brown adipocyte progenitors residing in skeletal muscle and white fat. *Proc Natl Acad Sci U S A*. Jan 4;108(1):143-8.

Seale P, Bjork B, Yang W, Kajimura S, Chin S, Kuang S, Scimè A, Devarakonda S, Conroe HM, Erdjument-Bromage H, Tempst P, Rudnicki MA, Beier DR, Spiegelman BM. (2008) PRDM16 controls a brown fat/skeletal muscle switch. *Nature*. Aug 21;454(7207):961-7.

Seale P, Conroe HM, Estall J, Kajimura S, Frontini A, Ishibashi J, Cohen P, Cinti S, Spiegelman BM. (2011) PRDM16 determines the thermogenic program of subcutaneous white adipose tissue in mice. *J Clin Invest*. Jan;121(1):96-105.

Shanks N, Greek R, Greek J. (2009) Are animal models predictive for humans? *Philos Ethics Humanit Med*. Jan 15;4:2.

Sharma NS, Nagrath D, Yarmush ML. (2011) Metabolic profiling based quantitative evaluation of hepatocellular metabolism in presence of adipocytes derived extracellular matrix. *PLoS One*. 6(5). Epub 2011 May 16.

Singh A, Zhan J, Ye Z, Elisseeff JH. (2013) Modular Multifunctional Poly(ethylene glycol) Hydrogels for Stem Cell Differentiation. *Adv. Funct. Mater*. 23(5):575-582.

Smih F, Rouet P, Lucas S, Mairal A, Sengenes C, Lafontan M, Vaulont S, Casado M, Langin D. (2002) Transcriptional regulation of adipocyte hormone-sensitive lipase by glucose. *Diabetes.* Feb;51(2):293-300.

Stanford KI, Middelbeek RJ, Townsend KL, An D, Nygaard EB, Hitchcox KM, Markan KR, Nakano K, Hirshman MF, Tseng YH, Goodyear LJ. (2013) Brown adipose tissue regulates glucose homeostasis and insulin sensitivity. *J Clin Invest*. Jan;123(1):215-23.

Steculorum SM, Ruud J, Karakasilioti I, Backes H, Engström Ruud L, Timper K, Hess ME, Tsaousidou E, Mauer J, Vogt MC, Paeger L, Bremser S, Klein AC, Morgan DA, Frommolt P, Brinkkötter PT, Hammerschmidt P, Benzing T, Rahmouni K, Wunderlich FT, Kloppenburg P, Brüning JC. (2016) AgRP Neurons Control Systemic Insulin Sensitivity via Myostatin Expression in Brown Adipose Tissue. *Cell*. Mar 24;165(1):125-38.

Stefl B, Janovská A, Hodný Z, Rossmeisl M, Horáková M, Syrový I, Bémová J, Bendlová B, Kopecký J. (1998) Brown fat is essential for cold-induced thermogenesis but not for obesity resistance in aP2-Ucp mice. *Am J Physiol*. Mar;274(3 Pt 1):E527-33.

Stevens MM and George JH. (2005) Exploring and engineering the cell surface interface. *Science*. Nov 18;310(5751):1135-8.

Stock MJ and Rothwell NJ. (1983) Role of brown adipose tissue thermogenesis in overfeeding: a review. *J R Soc Med*. Jan;76(1):71-3.

Stosich MS, Bastian B, Marion NW, Clark PA, Reilly G, Mao JJ. (2007) Vascularized adipose tissue grafts from human mesenchymal stem cells with bioactive cues and microchannel conduits. *Tissue Eng*. Dec;13(12):2881-90.

Timmons JA, Wennmalm K, Larsson O, Walden TB, Lassmann T, Petrovic N, Hamilton DL, Gimeno RE, Wahlestedt C, Baar K, Nedergaard J, Cannon B. (2007) Myogenic gene

expression signature establishes that brown and white adipocytes originate from distinct cell lineages. *Proc Natl Acad Sci U S A*. Mar 13;104(11):4401-6. Epub 2007 Mar 5.

Tiraby C, Tavernier G, Lefort C, Larrouy D, Bouillaud F, Ricquier D, Langin D. (2003) Acquirement of brown fat cell features by human white adipocytes. *J Biol Chem*. Aug 29;278(35):33370-6.

To MS, Aromataris EC, Castro J, Roberts ML, Barritt GJ, Rychkov GY. (2010) Mitochondrial uncoupler FCCP activates proton conductance but does not block store-operated Ca(2+) current in liver cells. *Arch Biochem Biophys*. Mar 15;495(2):152-8.

Ursino MG, Vasina V, Raschi E, Crema F, De Ponti F. (2009) The beta3-adrenoceptor as a therapeutic target: current perspectives. *Pharmacol Res*. Apr;59(4):221-34.

von Heimburg D, Zachariah S, Heschel I, Kühling H, Schoof H, Hafemann B, Pallua N. (2001) Human preadipocytes seeded on freeze-dried collagen scaffolds investigated in vitro and in vivo. *Biomaterials*. Mar;22(5):429-38.

van Marken Lichtenbelt WD, Vanhommerig JW, Smulders NM, Drossaerts JM, Kemerink GJ, Bouvy ND, Schrauwen P, Teule GJ. (2009) Cold-activated brown adipose tissue in healthy men. *N Engl J Med*. Apr 9;360(15):1500-8.

van Marken Lichtenbelt WD and Schrauwen P. (2011) Implications of nonshivering thermogenesis for energy balance regulation in humans. *Am J Physiol Regul Integr Comp Physiol*. 301: R285–R296.

Virtanen KA, Lidell ME, Orava J, Heglind M, Westergren R, Niemi T, Taittonen M, Laine J, Savisto NJ, Enerbäck S, Nuutila P. (2009) Functional brown adipose tissue in healthy adults. *N Engl J Med*. Apr 9;360(15):1518-25.

Whittle AJ, Carobbio S, Martins L, Slawik M, Hondares E, Vázquez MJ, Morgan D, Csikasz RI, Gallego R, Rodriguez-Cuenca S, Dale M, Virtue S, Villarroya F, Cannon B, Rahmouni K, López M, Vidal-Puig A. (2012) BMP8B increases brown adipose tissue thermogenesis through both central and peripheral actions. *Cell*. May 11;149(4):871-85.

Williams CG, Malik AN, Kim TK, Manson PN, Elisseeff JH. (2005) Variable cytocompatibility of six cell lines with photoinitiators used for polymerizing hydrogels and cell encapsulation. *Biomaterials*. Apr;26(11):1211-8.

Wong WT, Tian XY, Xu A, Yu J, Lau CW, Hoo RL, Wang Y, Lee VW, Lam KS, Vanhoutte PM, Huang Y. (2011) Adiponectin is required for PPARgamma-mediated improvement of endothelial function in diabetic mice. *Cell Metab*. Jul 6;14(1):104-15.

Wu I, Nahas Z, Kimmerling KA, Rosson GD, Elisseeff JH. (2012) An injectable adipose matrix for soft-tissue reconstruction. *Plast Reconstr Surg*. Jun;129(6):1247-57.

Yadav H, Quijano C, Kamaraju AK, Gavrilova O, Malek R, Chen W, Zerfas P, Zhigang D, Wright EC, Stuelten C, Sun P, Lonning S, Skarulis M, Sumner AE, Finkel T, Rane SG. (2011) Protection from obesity and diabetes by blockade of TGF-β/Smad3 signaling. *Cell Metab*. Jul 6;14(1):67-79.

Yang F, Williams CG, Wang DA, Lee H, Manson PN, Elisseeff J. (2005) The effect of incorporating RGD adhesive peptide in polyethylene glycol diacrylate hydrogel on osteogenesis of bone marrow stromal cells. *Biomaterials*. Oct;26(30):5991-8.

Young P, Arch JR, Ashwell M. (1984) Brown adipose tissue in the parametrial fat pad of the mouse. *FEBS Lett*. Feb 13;167(1):10-4.

Zhou Z, Yon Toh S, Chen Z, Guo K, Ng CP, Ponniah S, Lin SC, Hong W, Li P. (2003) Cidea-deficient mice have lean phenotype and are resistant to obesity. *Nat Genet*. Sep;35(1):49-56.

CURRICULUM VITAE

ANNEMARIE MCCARTNEY

PERSONAL DATA

Born in Cincinnati, Ohio on September 15, 1985.

amm@jhmi.edu

EDUCATION

07/2007 – Present Johns Hopkins University Baltimore, MD
School of Medicine
- MD-PhD Candidate

08/2003 – 05/2007 Miami University Oxford, OH
Major: Zoology, Minor: Neuroscience
- Earned Bachelor of Science degree.
- Graduated with Honors with Distinction.
  - This achievement required proposal, development, and completion of a large-scale research project.
- Gave commencement speech at College of Arts and Science graduation ceremony.

EMPLOYMENT

08/2013 – 03/2014 USSF Soccer Referee Baltimore, MD
Grade 8 Certification
- Officiated multiple soccer games per week for youth aged 7 – 18 at the recreational, high school, and tournament levels.

02/2004 – 05/2007 Student Health Services, Miami University Oxford, OH
Peer Health Educator
- Responsible for the creation and facilitation of health awareness programs on campus.
- President of student organization, August 2006 – May 2007
  - Secured funding for the 2006-2007 academic year.

RESEARCH ACTIVITIES

07/2011 – 06/2014 Elisseeff Lab Baltimore, MD

- Completed Ph.D thesis work, differentiating rat and human adipose-derived stem cells to brown adipose tissue in an optimized 3-dimensional synthetic hydrogel construct. Research on brown adipose was a new area of study for the lab, and several other students went on to work on branches of this project.
- Optimized lab protocol for using the Seahorse Extracellular Flux Analyzer to study cells grown in monolayer, and developed new protocol to use the machine to measure respiration of cells grown in 3-dimensional synthetic constructs.

PRESENTATIONS

- McCartney, AM. What's My Motivation? Encouraging weight loss in overweight and obese adolescents. Oral presentation at Adolescent Medicine Grand Rounds, Johns Hopkins Children's Center. April 22, 2016.

- McCartney, AM, VL Abejuela, and LG Isaacson. TrkB-immunoreactive cells in the intermediolateral cell column of the spinal cord: effects of exogenous nerve growth factor. Poster presentation at the Society for Neuroscience annual meeting. October 15, 2006.

- McCartney, AM, et al. The effect of weight-supported exercise on recovery of locomotor function after spinal cord contusion injury in the rat. Oral presentation at the Ohio Student Research Forum of the Ohio Science and Engineering Alliance. August 11, 2006.

- McCartney, AM, VL Abejuela, and LG Isaacson. Effects of *in vivo* NGF infusion on trkB immunoreactivity in the rat spinal cord. Poster presentation at the Ohio Miami Valley regional meeting of the Society for Neuroscience. May 8, 2006.

PUBLICATIONS

- Reid B, Afzal JM, McCartney AM, Abraham MR, O'Rourke B, Elisseeff JH. 2013. Enhanced tissue production through redox control in stem cell-laden hydrogels. *Tissue Eng Part A*. Sep;19(17-18):2014-23.

- McCartney, AM, Abejuela VL, Isaacson LG. 2006. TrkB immunoreactive cells in the intermediolateral cell column of the spinal cord: effects of exogenous nerve growth factor. Program No. 126.20. *2006 Abstr. Viewer/Itinerary Planner*. Atlanta, GA: Society for Neuroscience, 2006. Online.

- McCartney, AM, Abejuela VL, Isaacson LG. 2008. Characterization of trkB immunoreactive cells in the intermediolateral cell column of the rat spinal cord. *Neurosci Lett* 440 (2): 103-108.

- President's Distinguished Service Award, Miami University, April 2007

  - Awarded to 15 students who are nominated by faculty for their service to the campus and community.

- Undergraduate Student Travel Award, Faculty for Undergraduate Neuroscience, July 2006.

  - Awarded to around 20 top undergraduate neuroscientists nationwide to offset the cost of presenting their research at the annual meeting of the Society for Neuroscience.

- Dean's Scholar research award, Miami University, 2006 – 2007 academic year

  - Based on a research proposal submitted in junior year, 30 students are selected to be Dean's Scholars, and both the student and mentor receive a stipend towards conducting independent research in the senior year.

- Scholar Leader Community award, Miami University, 2005 – 2006 academic year

  - The Scholar Leader Community selects 75 students to live in a residential living-learning community for one year, after a multi-stage application and selection process. Students live in endowed rooms that provide partial scholarships.

- Undergraduate Summer Scholars research internship, Miami University, May 2005 – July 2005

  - Open to sophomore and junior students, up to 100 awards are granted based on merit of a research proposal, which is to be conducted full-time during the summer academic period. This program provides a fellowship award, project expense stipend, and tuition waiver to the student and an expense stipend to the mentor.

- Harrison Scholarship, Miami University, 2003 – 2007 academic years.

  - The most prestigious scholarship offered by Miami University, it awards full tuition, room, and board for four years, valued at well over $100,000. Thousands of applicants compete for around 25 scholarships, and winners typically have scored over 1470 on the SAT or over 33 on the ACT, rank in the top 1-3% of their class, and have a record of outstanding academic achievement and extracurricular involvement. A full-time faculty adviser is dedicated to Harrison students, and the group meets to discuss books, encourage scholarship, and design and attend service trips.

- National Merit Scholarship award winner, 2003.

  - Single payment scholarship of $2500. Out of the 1.5 million students who meet entry requirements, about 7,400 students receive a Merit

Scholarship. Students must earn a qualifying score on the PSAT and SAT, write an essay, have a record of high academic achievement, and be recommended by a school official.

- Valedictorian, Campbell County High School, 2003.

  - Highest ranked GPA in graduating class of over 300 students.

VOLUNTEERISM

- Medical Student Member, B'More Fit For Kids, 02/2016–present

  - Work twice monthly with second year pediatric residents to teach children aged 5-10 about healthy eating, introduce them to new foods, and lead them in playful physical activity.

- Adult Leader, "Central Students: Varsity" at Central Christian Assembly, 02/2015 – 07/2015.

  - Served on Sunday evenings as an adult leader of the youth group for high-school aged teens, leading in worship and songs and discussing challenges that the kids experienced in their daily lives.

- College Ambassador, Miami University College of Arts & Sciences, 2006–2007 academic year.

  - Represented the student body, alongside the Office of Admission, at university-sponsored events and discussed life at Miami with prospective students and their parents. Ambassadors are nominated by faculty due to academic achievement and extracurricular accomplishments.